Building and Environment 219 (2022) 109123

Contents lists available at ScienceDirect

Building and Environment

journal homepage: www.elsevier.com/locate/buildenv

Overall uncertainty analysis of zonal indoor air temperature measurement in an in-use office building

Catalina Giraldo-Soto [a,*], Laurent Mora [b], Aitor Erkoreka [a], Irati Uriarte [a], Pablo Eguia [c]

[a] ENEDI Research Group, Energy Engineering Department, Faculty of Engineering of Bilbao, University of Basque Country UPV/EHU. Pl. Ingeniero Torres Quevedo 1, 48013, Bilbao, Spain
[b] I2M - Institute of Mechanics and Engineering, University of Bordeaux CNRS (UMR 5295), Site ENSAM, Esplanade des Arts et Métiers, 33400, Talence, France
[c] Department of Mechanical Engineering, Heat Engines and Fluid Mechanics, School of Industrial Engineering, University of Vigo, 36310, Vigo, Spain

ARTICLE INFO

Keywords:
Indoor air temperature
Thermal zone
Uncertainty
Measurement
Monitoring system

ABSTRACT

Generally, studies where the zonal indoor air temperature is measured only consider the manufacturers' sensor accuracy to determine the overall Temperature Uncertainty (U_T), without considering other sources of uncertainties that affect the indoor air temperature measurement of a thermal zone within a building. Thus, in this research, the definition and estimation method of the overall Temperature Uncertainty (U_T) has been developed, together with a decoupling method to obtain the Temperature's Spatial Uncertainty ($U_{T(SP)}$), in which all causes of uncertainty regarding the temperature measurement are included, except the Temperature Sensor Uncertainty ($U_{T(S)}$). Using the measurements of the indoor air temperature from sensors installed randomly in four offices of an in-use tertiary building, the developed statistical analysis has been applied to estimate and decouple the overall indoor air Temperature Uncertainty (U_T) of each monitored office. Each studied thermal zone represents a different office typology composed of divisions with different volumes that allow their classification.

The first study carried out was the estimation of the experimental accuracy by estimating the Temperature Sensor Uncertainty ($U_{T(S)}$), including both the sensor uncertainty plus the monitoring system uncertainty in this value. This first study has allowed us to discover the importance of the estimation of the Temperature Sensor Uncertainty ($U_{T(S)}$) when installing a monitoring system, inasmuch as the experimental accuracy could be different from the manufacturer's accuracy, as reflected in the results of this research.

Secondly, based on the developed statistical method, for each of the monitored thermal zones, the overall zonal indoor air Temperature Uncertainty (U_T) is estimated in order to finally decouple it into the Temperature Sensor Uncertainty ($U_{T(S)}$) and Temperature's Spatial Uncertainty ($U_{T(SP)}$). The decoupling results show that, depending on the office typology, the percentage weight of the Temperature Sensor Uncertainty ($U_{T(S)}$) only represents between 5% and 11% of the overall zonal indoor air Temperature Uncertainty (U_T).

1. Introduction

Buildings are currently responsible for 40% of energy consumption, 36% of CO_2 emissions, and in addition, 35% of the buildings in the EU are over 50 years old, where 75% of the building stocks are energetically inefficient, and only 0.4–1.2% (depending on the country) of the building stock is renovated every year [1]. The European non-residential building stock (m^2) represents 25%, of which 23% are offices similar to the ones studied in this research, which make up the second-largest category of the total non-residential floor space [2].

In November 2017, the European Parliament and the Council reviewed the EU Emissions Trading System for the post-2020 period. This reviewed agreement was adopted in March 2018 [3]. The European long-term 2050 policies on climate currently have the reduction of domestic CO_2 emissions by 40%, 60% and 80% below 1990 levels by 2030, 2040, and 2050, respectively, as their target [3]. These indicators show the importance of moving forward to improve the design and evaluation of the retrofitting and construction of the building stock, where the office stock is an important sector to improve energy efficiency.

The reliable measurement of the zonal indoor air temperature, among others, plays an important role in efficiently operating in-use residential and tertiary buildings. It is common to have a thermostat per thermal zone of a building to represent the zonal indoor air tem-

* Corresponding author.
E-mail address: catalina.giraldo@ehu.eus (C. Giraldo-Soto).

https://doi.org/10.1016/j.buildenv.2022.109123
Received 4 January 2022; Received in revised form 16 April 2022; Accepted 19 April 2022
Available online 23 April 2022

Acronyms

°C	Degrees Celsius
AHSRAE	American Society of Heating, Refrigerating & Air-Conditioning Engineers
A2PBEER	Affordable and Adaptable Public Buildings through Energy Efficient Retrofitting
CWS	Compact Workspace
DF	Division Factor
DF_{OT}	Division Factor of an Office Typology
dv_i	Volume Differential
EU	Europe Union
F0	Ground Floor
F1	Floor One
F2	Floor Two
F3	Floor Three
g	Number of dv_i in an Office Typology volume
GUM	Guide to the Expression of Uncertainty in Measurement
hg	High Level
HTC	Heat Transfer Coefficient
HVAC	Heating Ventilation and Air Conditioning
ISO	International Organization for Standardisation
k	Coverage Factor
K	Kelvin
lw	Low Level
md	Medium Level
m^2	Square Meters
Max	Maximum
Min	Minimum
MCS	Monitoring and Controlling System
MMS	Mobile Monitoring System
MS	Monitoring Systems
μ	Mean
$\overline{\mu}$	Global Mean or Mean of the Sample
μ_{t_j}	Mean of Temperature Differentials for each Instant of Time
n	Number of Workspaces in an Office Typology
N	Number of Instants of Times or Sample Size
N_{CWS}	Number of Compact Workspaces in an Office Typology
N_{OWS}	Number of Open Workspaces an in Office Typology
OT	Office Typology
OT1	Office Typology One
OT2	Office Typology Two
OT3	Office Typology Three
OT4	Office Typology Four
OWS	Open Workspace
OWSR	Open Workspace Ratio
p	Number of T_{dv_i} in an Office Typology for each t_j
ppm	Parts per million
q	Number of T_{dv_i} in a Workspace for each t_j
RH	Relative Humidity
R_S	Sensor Ratio or Ratio of Mean Variance associated to Sensor Uncertainty with respect to Mean Variance associated to Temperature Uncertainty
R_{Sp}	Spatial Ratio or Ratio of Mean Variance associated to Temperature's Spatial Uncertainty with respect to Mean Variance associated to Temperature Uncertainty
RTU	Remote Terminal Unit Standard Deviation
σ^2	Variance
$\overline{\sigma}$	Mean Standard Deviation of the Sample
$\overline{\sigma^2}$	Mean-Variance of the Sample
$\overline{\sigma_{(S)}}$	Mean Standard Deviation of the Sample associated with Sensor Uncertainty
$\overline{\sigma^2_{(S)}}$	Mean-Variance of the Sample associated with Sensor Uncertainty
$\overline{\sigma_{(SP)}}$	Mean Standard Deviation of the Sample associated to Temperature's Spatial Uncertainty
$\overline{\sigma^2_{(SP)}}$	Mean-Variance of the Sample associated to Temperature's Spatial Uncertainty
σ_{t_j}	Standard Deviation of Temperature Differentials for each Instant of Time
$\sigma^2_{t_j}$	Variance of Temperature Differentials for each Instant of Time
$\sigma^2_{t_{j(S)}}$	Variance of Temperature Differentials for each Instant of Time associated with Sensor Uncertainty
$\sigma^2_{t_{j(SP)}}$	Variance of Temperature Differentials for each Instant of Time associated with Temperature's Spatial Uncertainty
SEM	Standard Error of the Mean
T_a	Average Temperature
$(T_a)_{OT}$	Average Temperature of Office Typology volume
$(T_a)_{WS}$	Average Temperature of Workspace volume
T_{dv_i}	Sensor Temperature Measurements of a Volume Differential (dv_i)
T_{in}	Indoor Air Temperature
t_j	Instant of Time (j = 1, …,N)
θ_{dv_i}	Temperature Differential
$(\theta_{dv_i})_{vw}$	Temperature Differential concerning the Volume-Weighted Temperature of an Office Typology
$(\theta_{dv_i})_a$	Temperature Differential concerning the Average Temperature of a Workspace volume
TT	Tripod Together
T_{vw}	Volume-Weighted Temperature
$(T_{vw})_{range}$	95% confidence range within which the representative volume-weighted temperature of a thermal zone lies
$(T_{vw})_{OT}$	Volume-Weighted Temperature of Office Typology
U	Standard Uncertainty
UPV/EHU	University of the Basque country
$\overline{U}$	Expanded Uncertainty
U_T	Temperature Uncertainty or Overall Temperature Uncertainty
$U_{T_{(SP)}}$	Temperature's Spatial Uncertainty
$U_{T(S)}$	Experimental Sensor Uncertainty of Temperature Measurement or Temperature Sensor Uncertainty
V_{OT}	Volume of Office Typology
V_{OWS}	Volume of Open Workspace
V_{WS}	Volume of Workspace
WS	Workspace
y	Number of dv_i in a Workspace volume
Z	Number of temperature measurements (T_{dv_i} or θ_{dv_i}) in each t_j in an OT ($Z = p$) or a WS ($Z = q$) volume

perature of each thermal zone. Indoor Air Temperature (T_{in}) is a physical variable studied and analysed in multiple scientific fields of buildings. These include tests related to indoor climate, user comfort, ventilation models, Heating, Ventilation and Air Conditioning (HVAC) control and building energy performance evaluation. The indoor air temperature is not only a physical variable that intervenes in user comfort and the optimisation of the building sub-systems but also favours the revitalisation and enhancement of the historical heritage [4] for which specific monitoring systems have been developed where indoor air temperature plays an important role [5].

Many publications deal with zonal indoor air temperature, which plays a key role in the studies of buildings. For example, it is currently

possible to find around 84,554 results concerning indoor temperature in buildings on science direct [6]. In the same way, the International Organization for Standardization (ISO) and the American Society of Heating, Refrigerating & Air-Conditioning Engineers (AHSRAE) state in their standards and handbooks that the T_{in} of buildings and its subsystems is an important physical variable used to develop procedures, methodologies and calculations.

For example, the ISO 52016–1:2017 [7] assumes "the air temperature is uniform throughout the room or zone" for thermal zones heating and cooling load calculation, "applicable to buildings at the design stage, to new buildings after construction and existing buildings in the use phase". Even if the ISO 52016–1:2017 should be valid for in-use buildings energy behaviour analysis, the requirements about the measurement uncertainty of indoor air temperature of thermal zones are not defined. Similarly, the ASHRAE Fundamentals Handbook 2021 [8] in Chapter 19, "Energy estimating and Modelling methods", estimates the indoor air temperature of thermal zones as a unique value considering it is thoroughly mixed or uniform within the thermal zone. In this chapter, at the same time, it is stated that "A limitation of many energy-estimating programs is the assumption that air within thermal zones is fully mixed …". Likewise, no reference to the uncertainty estimation of the zonal indoor air temperatures is present in this document. Even in chapter 38, "Measurements and instruments", no reference to the uncertainty associated with a thermal zone's indoor air temperature is exposed. This chapter is limited to presenting the approximate accuracy of the different sensors used to measure temperature for both gases and liquids. Finally, the ASHRAE HVAC Applications Handbook 2019 [9] in its chapter 42, "Building energy and water monitoring", only refers to a stated indoor air temperature accuracy of ±0.60 °C (in this value, only the sensor accuracy is considered).

In research works where thermal zone energy simulation models are calibrated against indoor air temperature measurements, it is common that a single sensor represents the indoor air temperature of a thermal zone, considering the sensor accuracy as the measurement uncertainty; this is the case of [10]. In Ref. [11], a retrofitted Victorian end-terrace whole house is tested within a controlled climatic chamber to estimate its envelope Heat Transfer Coefficient (HTC). The indoor air temperature of this tested building is measured in several rooms with ±0.10 °C accuracy temperature sensors; the arithmetic mean of all those measurements is used as the building indoor air temperature for HTC calculation purposes. The building is considered as a unique thermal zone for this analysis, and the standard deviation of the indoor arithmetic mean and the outdoor air temperature is used to estimate the HTC uncertainty by error propagation. However, the considered thermal zone indoor air temperature uncertainty is neither defined nor estimated. In Ref. [12], the reliability of the HTC estimation through the co-heating test [13] method is analysed in detail. In Ref. [12], a specific section regarding the analysis of the indoor air temperature uncertainty of the tested building (again, the whole building is considered as a unique thermal zone) is developed. Here, it is stated that even if the accuracy of the sensors used for measuring the indoor air temperature is ±0.20 °C, due to the variability of the indoor air temperature between the different rooms of the building, they assume a ±1 °C uncertainty for the indoor to outdoor air temperature difference. Again, a knowledge gap is evidenced regarding estimating the overall uncertainty of the indoor air temperature in thermal zones where there is a spatial and temporal variability of the temperature. Likewise, in Ref. [14], thermal comfort experiments were carried out within a climatic chamber where four indoor air temperature sensors measured the indoor air temperature with a ±0.20 °C accuracy. These air temperature measurements were used to prove that during the 90 min that took each comfort test, the air temperature was stable within the selected set-point temperature. Thus, together with the set-point of each test, the measured mean air temperature of each test plus/minus the Standard Error of the Mean (SEM) is given. The SEM is just used as a statistic parameter to check the stability of the indoor air temperature during each test. Again, even if they had four air temperature measurements within the monitored thermal zone, no overall uncertainty of the indoor air temperature was estimated.

Taking into account the importance of properly estimating the overall Uncertainty (U_T) value for the indoor air temperature measurements of thermal zones within a building, this paper focuses on developing a statistical method that permits it to be defined and quantified. The construction of this estimator is the main aim of this research work. Thus, the proposed analysis is developed on a practical basis for four offices with different cardinal orientations, divisions, volumes and geometries of a tertiary in-use building. In this way, it is possible to compare the overall uncertainty of the T_{in} measurement in the studied thermal zones with the sensor manufacturer's accuracy. It will therefore permit us to quantify and understand to what extent the indoor air temperature measurement's overall uncertainty of the monitored thermal zones is underestimated when only the manufacturers' accuracy is considered as the overall uncertainty of the measure.

2. Method

This section starts with the state of the art of uncertainty analysis methods and the developed methodology is then described for the following analysis:

- Temperature Sensor Uncertainty ($U_{T(S)}$) analysis: the uncertainty associated to systematic errors of the air temperature sensors and monitoring system is estimated experimentally so as to be compared with the manufacturer's accuracy of air temperature sensors.
- Temperature Uncertainty (U_T) analysis: this overall uncertainty estimation for the indoor air temperature in different thermal zones is performed experimentally. In this estimation, all uncertainty sources of the zonal indoor air temperature measurement are considered (systematic and random errors).
- Temperature's Spatial Uncertainty ($U_{T_{(SP)}}$) analysis: the uncertainty associated with random errors is estimated through an analytical procedure. For this, the Temperature Uncertainty (U_T) of the zonal indoor air is decoupled into the uncertainty associated with systematic errors (Temperature Sensor Uncertainty ($U_{T(S)}$) and the uncertainty associated with random errors (Temperature's Spatial Uncertainty ($U_{T_{(SP)}}$), considering both uncertainties are independent of each other.

The statistical method for estimating the Temperature Uncertainty (U_T) and the Temperature Sensor Uncertainty ($U_{T(S)}$) is the same, so it is first introduced as a general uncertainty analysis method at the start of subsection 2.1. Then the specific application of the method to each of these two cases is detailed within the subsection 2.2. Furthermore, this section develops a classification method for office typologies in order to make the results of this research extendable to similar office typologies.

2.1. State of the art of uncertainty analysis methods

The theoretical framework of the methodology carried out for the statistical analysis of the data to estimate the uncertainty is explained in this section. Data must be formed by experimental observations whose bell-shaped distribution is best represented by the normal distribution, also called the Gaussian distribution ([15,16]), where, for a sample composed of N subsamples with Z measures per subsample, it is possible to obtain the Mean (μ), the Variance (σ^2) and the Standard Deviation (σ) for each subsample (Z values), as well as the Global Mean ($\overline{\mu}$), Mean-Variance ($\overline{\sigma^2}$) and Mean Standard Deviation ($\overline{\sigma}$) of the sample (N values).

In addition, for samples with a normal distribution centred on the $\overline{\mu}$ and $\overline{\sigma}$ values, it is known a priori that 68% of the population falls within the interval $\overline{\mu} \pm \overline{\sigma}$. Measurements involve uncertainties, where repeated

measurements give an indication of the measurement uncertainty through the dispersion in its measured values. In the case of independent observation series of 30 or more, the evaluation of uncertainty by statistical analysis is called Type A evaluations based on the GUM method [16].

In the statistical analysis of the Type A assessment, the sample's Mean Standard Deviation ($\overline{\sigma}$) reflects the uncertainty value, where the Standard Uncertainty (U) is the measurement uncertainty expressed in terms of a sample's Mean Standard Deviation ($U = \overline{\sigma}$). If the U value is multiplied by a Coverage Factor (k) in a Type A evaluation, an "'Expanded Uncertainty" is obtained, which is expected to be within the 95% confidence level interval if the k-value is equal to 2 ($\overline{U} = 2\overline{\sigma}$), or 99% if it is equal to 3 ($\overline{U} = 3\overline{\sigma}$) [16]. When there are fewer than 30 repeated measurements, the appropriate k-value is based on the Student t-distributions [16].

In this manuscript, the overall Expanded Uncertainty ($\overline{U}$) value of the zonal Indoor Air Temperature (T_{in}) is called "Temperature Uncertainty (U_T)", with a U value multiplied by a k-value equal to 2. In addition, there are two different contributions of uncertainties, one due to systematic error (identified in this manuscript as Temperature Sensor Uncertainty ($U_{T(S)}$), and another due to random fluctuations (identified in this manuscript as Temperature's Spatial Uncertainty ($U_{T(SP)}$), both estimated as Expanded Uncertainties ($\overline{U}$) and considered to be independent of each other.

2.2. Uncertainty analysis method

2.2.1. Definition and estimation method of the zonal indoor air temperature uncertainty

There is a discrepancy between the real representative air temperature value of a volume (or thermal zone) and the individual temperature measurements from sensors. It will never be possible to know with certainty the real value of a measure because its uncertainty is due to both systematic errors (which can be controlled and eliminated) and different errors from random causes (which cannot be controlled and eliminated). Thus, the overall uncertainty of the measurement could be estimated by combining uncertainties of the systematic and random errors.

In this research, when defining the overall zonal T_{in} Uncertainty, the uncertainty associated with the systematic error, is given by the sensor accuracy (which is usually given by the manufacturer) and by the monitoring system where the sensor is installed. On the other hand, within the random errors considered as part of the definition of the zonal overall T_{in} Uncertainty, different causes that produce temperature variability within a thermal zone are considered, such as vertical and horizontal temperature stratification and/or variation, user behaviour, the incidence of solar radiation, or effects produced by the ventilation and heating system, among others.

The uncertainty estimation method set out in this section can be applied to indoor and outdoor zonal air Temperature (T_{in} and T_{out}), indoor and outdoor zonal Carbon Dioxide concentration, zonal Relative Humidity (RH) and any intensive variable zonal measurement that has the characteristics of a Type A sample.

First, the methodology implemented to analyse the data collected from the experimental tests carried out in a tertiary in-use building [17] are shown. The building was monitored to collect temperature values in four different offices (or thermal zones) of the building in order to study the uncertainty of those zonal indoor air temperature measurements. Then, having introduced the general method for uncertainty estimation, the subsections developed are the following [17]:

- Application of the methodology to estimate the Temperature Sensor Uncertainty ($U_{T(S)}$) and the overall Temperature Uncertainty (U_T).
- Decoupling methodology to obtain the Temperature's Spatial Uncertainty ($U_{T(SP)}$).
- Thermal zone characterisation: Office Typologies (OT).

In the statistical study to estimate the zonal T_{in} measurement uncertainty, the samples should be the Instant of Times (t_j) with $j = 1, \ldots, N$. In each (t_j), different temperature values have been acquired from sensors installed on tripods at different heights (High (hg), Medium (md) and Low (lw)), which in turn were randomly located in different positions of each monitored thermal zone. These temperature values are the Sensor Temperature Measurements (T_{dv_i}), defined as a temperature value in a Volume Differential (dv_i) of a thermal zone, which, in turn, dv_i represents the volume where a temperature sensor is located. As a practical example, Table A2, Table A3, Fig. A1 and Fig. A2 show the four tested thermal zones of the tertiary building. Here, it can be seen that Floor 2 is composed of three thermal zones (namely OT1, OT2 and OT3), and Floor 3 is considered as a unique thermal zone (namely OT4). Each of the four thermal zones represents an Office Typology (OT) (thus, there could be several thermal zones or OT per floor). In this practical example, it can be seen that each OT is composed of several volumes called Workspaces (WS). Section 2.3 specifies the definitions of OT and WS.

Eq. (1) defines the OT volume (V_{OT}) as the sum of n volumes of the WS (V_{WS}) that makes up the OT. Eq. (2) defines the WS volume (V_{WS}) as the sum of y units of dv_i contained in each WS. Likewise, Eq. (3) shows the Average Temperature of the indoor air in an OT ($(T_a)_{OT}$) defined by the sum of p units of T_{dv_i} measurement in an OT divided by p. Also, Eq. (4) shows the Average Temperature of the indoor air in a WS ($(T_a)_{WS}$) defined by the sum of q units of T_{dv_i} measurement in a WS divided by q. Eq. (5) defines the Volume-Weighted Temperature of the indoor air in an OT ($(T_{vw})_{OT}$), which is calculated as the sum of the Average Temperature of the indoor air in each WS ($(T_a)_{WS}$) multiplied by its volume weight in the OT. The volume weight is equal to the WS Volume (V_{WS}) divided by the OT Volume (V_{OT}).

As stated previously, the samples of the experimental study carried out are composed of N Instants of Time (t_j), for which independent Z measurements of T_{dv_i} were collected from sensors located at different heights and positions; henceforth each t_j has Z unitis of T_{dv_i} measurements. The proposed statistical analysis was carried out to estimate the uncertainties associated with zonal T_{in} measurements, where these measurements shall be made up of T_{dv_i} values centred with respect to the Average Temperature (T_a) (of OT $(T_a)_{OT}$ or WS $((T_a)_{WS})$ or the Volume-Weighted Temperature (T_{vw}) (of OT $((T_{vw})_{OT})$ of the corresponding t_j; for which Eq. (6) or Eq. (7) is used in order to have a new temperature value in each sensor measurement point called, in this manuscript, Temperature Differential (θ_{dv_i}). From this point on, each Instant of Time (t_j) has Z new temperature values (the Temperature Differentials (θ_{dv_i}), which are centred on an Average Temperature (T_a) or Volume-Weighted Temperature (T_{vw}). For these new temperature values, the statistical uncertainty study is carried out to estimate the temperature measurement uncertainty.

Once the measured temperatures have been centred on the Average Temperature (T_a) or the Volume-Weighted Average Temperature (T_{vw}), the hypothesis that the centred instants of time are independent of each other can be considered [17]. Now that we are working with the centred temperature differentials, for each time instant, the variations of θ_{dv_i} are due to systematic and random variations of the indoor air temperature within the thermal zone. Furthermore, the data collected over a long span of time and having a large sample size ensures that the data collected follows a type A distribution [16].

In the case where there is only one sensor temperature measurement in a volume, the T_{dv_i} value cannot be centred concerning a reference temperature, so the proposed statistical analysis cannot be applied to those volumes.

$$V_{OT} = \sum_{j=1}^{n} V_{WS_j} = \sum_{i=1}^{g} dv_i \left[m^3\right] \quad (1)$$

$$V_{WS} = \sum_{i=1}^{y} dv_i \ [m^3] \quad (2)$$

where,

V_{OT}: OT Volume [m^3].
V_{WS}: WS Volume [m^3].
dv_i: Volume Differential contained in an OT or a WS [m^3].
g: Number of Volume Differentials in an OT volume.
y: Number of Volume Differentials in a WS volume.
n: Number of WS volumes contained in an OT.

$$(T_a)_{OT} = \sum_{i=1}^{p} \frac{T_{dvi}}{p} \ [K \text{ or } ^\circ C] \quad (3)$$

$$(T_a)_{WS} = \sum_{i=1}^{q} \frac{T_{dvi}}{q} \ [K \text{ or } ^\circ C] \quad (4)$$

where,

T_a: Average Temperature of a Volume for each t_j [K or °C].
$(T_a)_{OT}$: Average Temperature of an OT Volume for each t_j [K or °C]
$(T_a)_{WS}$: Average Temperature of a WS volume for each t_j [K or °C].
T_{dvi}: Sensor Temperature Measurement in certain dv_i for each t_j [K or °C].
p: Number of T_{dvi} measurement in an OT for each t_j.
q: Number of T_{dvi} measurement in a WS for each t_j.

$$(T_{vw})_{OT} = \frac{1}{V_{OT}} \sum_{j=1}^{n} V_{WS_j} \left(\frac{\sum_{i=1}^{q} (T_{dvi})_{WS_j}}{q} \right) = \frac{1}{V_{OT}} \sum_{j=1}^{n} V_{WS_j} (T_a)_{WS_j} \ [K \text{ or } ^\circ C] \quad (5)$$

where,

$(T_{vw})_{OT}$: Volume-Weighted Temperature of an OT for each t_j [K or °C].
$(T_{dvi})_{WS}$: Sensor Temperature Measurements (T_{dvi}) in a certain dv_i of a WS for each t_j [K or °C].

$$(\theta_{dv_i})_{vw} = T_{dvi} - (T_{vw})_{OT} \ [K \text{ or } ^\circ C] \quad (6)$$

where,

$(\theta_{dv_i})_{vw}$: Temperature Differential of a certain T_{dvi} concerning the Volume-Weighted Temperature of an OT for each t_j [K or °C].

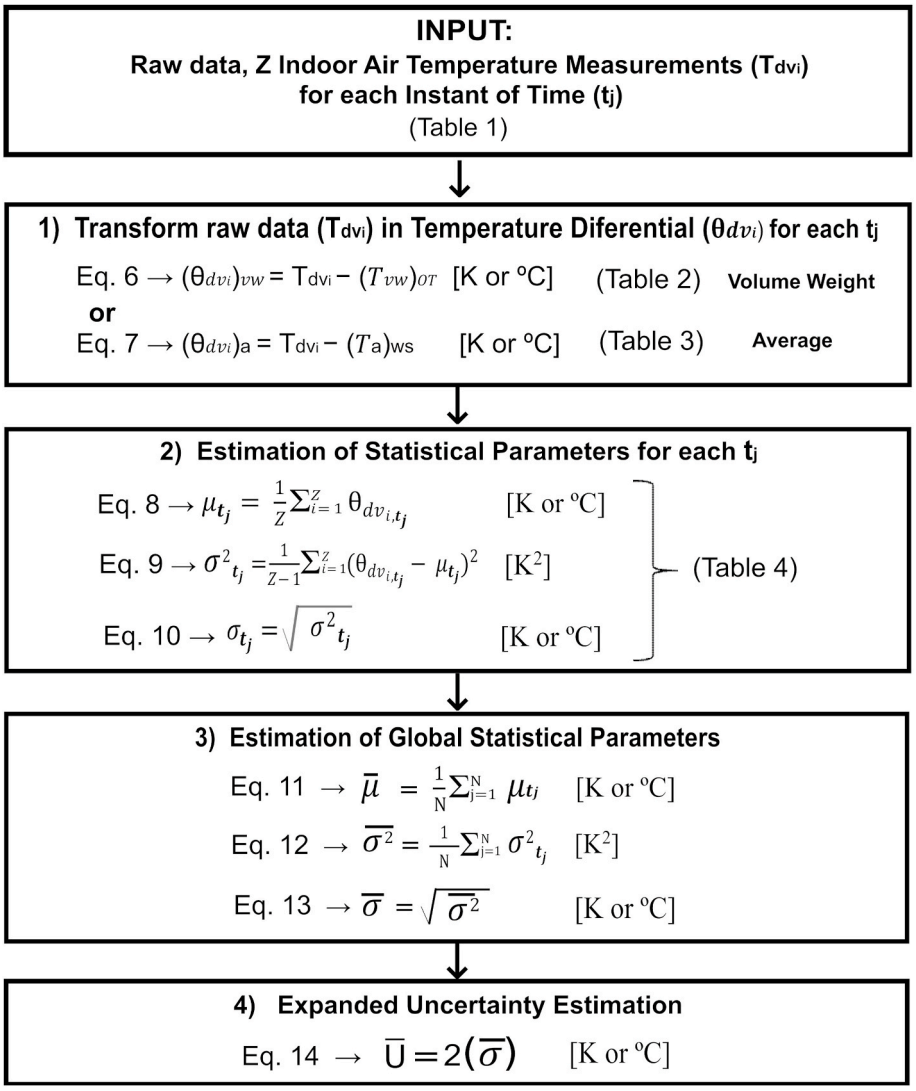

Fig. 1. Flowchart of the methodology to estimate the Expanded Uncertainty ($\bar{U}$) of the zonal indoor air temperature (T_{in}) measurement.

$$(\theta_{dv_i})_a = (T_{dvi})_{WS} - (T_a)_{WS} \text{ [K or °C]} \quad (7)$$

where,

$(\theta_{dv_i})_a$: Temperature Differential of a certain T_{dvi} concerning the Average Temperature of a WS for each t_j [K or °C].

$$\mu_{t_j} = \frac{1}{Z}\sum_{i=1}^{Z} \theta_{dv_i,t_j} \text{ [K or °C]} \quad (8)$$

$$\sigma^2_{t_j} = \frac{1}{Z-1}\sum_{i=1}^{Z} \left(\theta_{dv_i,t_j} - \mu_{t_j}\right)^2 \text{ [K}^2\text{]} \quad (9)$$

$$\sigma_{t_j} = \sqrt{\sigma^2_{t_j}} \text{ [K or °C]} \quad (10)$$

$$\overline{\mu} = \frac{1}{N}\sum_{j=1}^{N} \mu_{t_j} \text{ [K or °C]} \quad (11)$$

$$\overline{\sigma}^2 = \frac{1}{N}\sum_{j=1}^{N} \sigma^2_{t_j} \text{ [K}^2\text{]} \quad (12)$$

$$\overline{\sigma} = \sqrt{\overline{\sigma}^2} \text{ [K or °C]} \quad (13)$$

$$\overline{U} = 2(\overline{\sigma}) \text{ [K or °C]} \quad (14)$$

where,

θ_{dv_i,t_j}: Temperature Differential, defined by the difference of each T_{dv_i} concerning $(T_a)_{ws}$ or $(T_{vw})_{OT}$ for each t_j [K or °C].
μ_{t_j}: Mean of Temperature Differentials θ_{dv_i} for each t_j [K or °C].
$\sigma^2_{t_j}$: Variance of Temperature Differentials θ_{dv_i} for each t_j [K^2].
σ_{t_j}: Standard Deviation of Temperature Differentials θ_{dv_i} for each t_j [K or °C].
$\overline{\mu}$: Global Mean or Mean of N μ_{t_j} [K or °C].
$\overline{\sigma}^2$: Mean-Variance of N $\sigma^2_{t_j}$ [K^2].

$\overline{\sigma}$: Mean Standard Deviation of the sample, this value is associated with the Temperature Uncertainty estimation [K or °C].
Z: Number of T_{dv_i} measurement in an OT ($Z = p$) or a WS ($Z = q$) volume for each t_j.
N: Sample Size defined by the number of Instants of Time (t_j).

The steps carried out for the statistical analysis are shown in Fig. 1 and are detailed in Ref. [17]:

1) Transform the raw data of each time instant (t_j) (Table 1) in a centred Temperature Differential $(\theta_{dv_i})_{vw}$ (Eq. (6)) or $(\theta_{dv_i})_a$ (Eq. (7)), according to the volume type to be studied, V_{OT} or V_{ws}. Now, for each time instant (t_j), a new normal distribution N (μ, σ) with mean, μ, and standard deviation, σ (Tables 2 and 3), is obtained.
2) Calculate the statistical parameters for θ_{dv_i} values of each t_j: the mean (μ), standard deviation (σ) and Variance (σ^2) values, as well as maximum (Max) and minimum (Min) values, are obtained for each time instant (Table 4).

Table 1
Matrix of measured raw data for a sample composed of N t_j.

Temperature Measurement	Instant of Times (Sample)				
$\mathbf{Tdv_{i,t_j}}$ | $\mathbf{t_j}$	$(\mathbf{t_1})$	$(\mathbf{t_2})$	$(\mathbf{t_3})$	**…**	$(\mathbf{t_N})$
$\mathbf{Tdv_{1,t_j}}$	$Tdv_{1,1}$	$Tdv_{1,2}$	$Tdv_{1,3}$	…	$Tdv_{1,N}$
$\mathbf{Tdv_{2,t_j}}$	$Tdv_{2,1}$	$Tdv_{2,2}$	$Tdv_{2,3}$	…	$Tdv_{2,N}$
$\mathbf{Tdv_{3,t_j}}$	$Tdv_{3,1}$	$Tdv_{3,2}$	$Tdv_{3,3}$	…	$Tdv_{3,N}$
…	…	…	…	…	…
$\mathbf{Tdv_{Z,t_j}}$	$Tdv_{Z,1}$	$Tdv_{Z,2}$	$Tdv_{Z,3}$	…	$Tdv_{Z,N}$

Table 2
Matrix of centred data concerning $(T_{vw})_{OT}$ with a Normal Distribution N(μ, σ) for each t_j.

Temperature differentials	Instant of Times (Sample)				
$\left(\boldsymbol{\theta_{dv_{i,t_j}}}\right)_{vw}$ **(Eq. (6))**| $\mathbf{t_j}$	$(\mathbf{t_1})$	$(\mathbf{t_2})$	$(\mathbf{t_3})$	**…**	$(\mathbf{t_N})$
$\left(\boldsymbol{\theta_{dv_{1,t_j}}}\right)_{vw}$	$(\theta_{dv_{1,1}})_{vw}$	$(\theta_{dv_{1,2}})_{vw}$	$(\theta_{dv_{1,3}})_{vw}$	…	$(\theta_{dv_{1,N}})_{vw}$
$\left(\boldsymbol{\theta_{dv_{2,t_j}}}\right)_{vw}$	$(\theta_{dv_{2,1}})_{vw}$	$(\theta_{dv_{2,2}})_{vw}$	$(\theta_{dv_{2,3}})_{vw}$	…	$(\theta_{dv_{2,N}})_{vw}$
$\left(\boldsymbol{\theta_{dv_{3,t_j}}}\right)_{vw}$	$(\theta_{dv_{3,1}})_{vw}$	$(\theta_{dv_{3,2}})_{vw}$	$(\theta_{dv_{3,3}})_{vw}$	…	$(\theta_{dv_{3,N}})_{vw}$
…	…	…	…	…	…
$\left(\boldsymbol{\theta_{dv_{Z,t_j}}}\right)_{vw}$	$(\theta_{dv_{Z,1}})_{vw}$	$(\theta_{dv_{Z,2}})_{vw}$	$(\theta_{dv_{Z,3}})_{vw}$	…	$(\theta_{dv_{Z,N}})_{vw}$

Table 3
Matrix of centred data concerning $(T_a)_{WS}$ with a Normal Distribution N(μ, σ) for each t_j.

Temperature differentials	Instant of Times (Sample)				
$\left(\boldsymbol{\theta_{dv_{i,t_j}}}\right)_{a}$ **(Eq. (7))**| $\mathbf{t_j}$	$(\mathbf{t_1})$	$(\mathbf{t_2})$	$(\mathbf{t_3})$	**…**	$(\mathbf{t_N})$
$\left(\boldsymbol{\theta_{dv_{1,t_j}}}\right)_{a}$	$(\theta_{dv_{1,1}})_a$	$(\theta_{dv_{1,2}})_a$	$(\theta_{dv_{1,3}})_a$	…	$(\theta_{dv_{1,N}})_a$
$\left(\boldsymbol{\theta_{dv_{2,t_j}}}\right)_{a}$	$(\theta_{dv_{2,1}})_a$	$(\theta_{dv_{2,2}})_a$	$(\theta_{dv_{2,3}})_a$	…	$(\theta_{dv_{2,N}})_a$
$\left(\boldsymbol{\theta_{dv_{3,t_j}}}\right)_{a}$	$(\theta_{dv_{3,1}})_a$	$(\theta_{dv_{3,2}})_a$	$(\theta_{dv_{3,3}})_a$	…	$(\theta_{dv_{3,N}})_a$
…	…	…	…	…	…
$\left(\boldsymbol{\theta_{dv_{Z,t_j}}}\right)_{a}$	$(\theta_{dv_{Z,1}})_a$	$(\theta_{dv_{Z,2}})_a$	$(\theta_{dv_{Z,3}})_a$	…	$(\theta_{dv_{Z,N}})_a$

Table 4
Matrix of statistical parameters of the Normal Distributions N(μ, σ) for each t_j.

Statistical Parameters | $\mathbf{t_j}$	$(\mathbf{t_1})$	$(\mathbf{t_2})$	$(\mathbf{t_3})$	**…**	$(\mathbf{t_N})$
$\boldsymbol{\mu_{t_j}}$ **(Eq. (8))**	μ_{t_1}	μ_{t_2}	μ_{t_3}	…	μ_{t_N}
$\boldsymbol{\sigma^2_{t_j}}$ **(Eq. (9))**	$\sigma^2_{t_1}$	$\sigma^2_{t_2}$	$\sigma^2_{t_3}$	…	$\sigma^2_{t_N}$
$\boldsymbol{\sigma_{t_j}}$ **(Eq. (10))**	σ_{t_1}	σ_{t_2}	σ_{t_3}	…	σ_{t_N}
$\mathbf{Max_{t_j}}$	Max_{t_1}	Max_{t_2}	Max_{t_3}	…	Max_{t_N}
$\mathbf{Min_{t_j}}$	Min_{t_1}	Min_{t_2}	Min_{t_3}	…	Min_{t_N}

3) Calculate the Global Mean ($\overline{\mu}$, Eq. (11)), Mean-Variance ($\overline{\sigma^2}$, Eq. (12)) and the Mean Standard Deviation ($\overline{\sigma}$, Eq. (13)) of the sample composed by N instants of time (t_j), based on the GUM method [16]; where the $\overline{\sigma}$ value is associated with the Temperature Uncertainty (U_T) of the zonal T_{in} measurement of the studied thermal zone.
4) Estimate the expanded Temperature Uncertainty (U_T), with a confidence interval of 95%, multiplying $\overline{\sigma}$ by k = 2, based on the GUM method [16]. All Uncertainty values estimated in this manuscript are Expanded Uncertainties.

These statistical parameters have been calculated on a practical basis to obtain the results of subsections 4.1 and 4.2 using Scispy-stats [18], Pandas libraries [19] and programming in Python [20].

2.2.2. *Temperature Sensor Uncertainty ($U_{T(S)}$) analysis for the Mobile Monitoring System (MMS)*

This analysis aims to obtain the experimental accuracy of the sensors plus the MMS. To estimate this experimental value, for each time instant, t_j, nineteen temperature measurements, T_{dvi}, have been obtained by installing the nineteen sensors together at a similar height in the same location of the same WS. The experimental accuracy of the sensors plus MMS, or the Temperature Sensor Uncertainty ($U_{T(S)}$), is given by the Expanded Uncertainty $2\overline{\sigma}$ value, as described in section 2.1. This is obtained from the temperature differentials, the $(\theta_{dv_i})_a$ (Eq. (7)) values of each temperature T_{dv_i} value for each t_j in the WS. The $U_{T(S)}$ (Eq. (14)) value represents the experimental accuracy of the sensor

measurements for a manufacturer's specific technology within a specific monitoring system [17].

2.2.3. Zonal indoor air temperature uncertainty (U_T) analysis for a monitored thermal zone

In this section, the methodology used to estimate the Temperature Uncertainty is also based on section 2.1, and the study has been carried out for four different OTs [17]. Here, sensors are randomly distributed throughout the volume of each thermal zone, as detailed in section 3. For estimating the U_T value for an OT, the temperature differential, $(\theta_{dv_i})_{vw}$ (Eq. (6)), must first be calculated for each temperature value T_{dv_i} of each t_j and then the statistical analysis of these $(\theta_{dv_i})_{vw}$ values must be done. The U_T value is calculated for the monitored OT using Eq. (14), which includes $U_{T(S)}$ and all the other uncertainty causes described in section 2.1.

2.2.4. Zonal indoor air temperature uncertainty (U_T) decoupling method to estimate the Temperature's Spatial Uncertainty ($U_{T_{(SP)}}$)

The previously obtained zonal indoor air Temperature Uncertainty (U_T) value includes both $U_{T_{(S)}}$ and $U_{T_{(SP)}}$ of the monitored thermal zone.

Decoupling the U_T value, it is possible to estimate the $U_{T_{(SP)}}$ value based on the Mean-Variances (see Eq. (12)), calculated in subsections 2.2.2 and 2.2.3, used to estimate $U_{T_{(S)}}$ and U_T respectively. Fig. 2 shows the flowchart for the application of the Temperature Uncertainty (U_T) decoupling method. Thus, through the analytical method of the Mean-Variance sum presented in (Eq. (19)), it is possible to decouple the Temperature Uncertainty (U_T) since:

- The $U_{T(S)}$ value is independent of the rest of the causes of temperature uncertainty, $U_{T_{(SP)}}$.
- Both uncertainties ($U_{T(S)}$ and $U_{T_{(SP)}}$) make up the Temperature Uncertainty (U_T) value.
- The Mean-Variance $\overline{\sigma_T^2}$ associated to U_T is the sum of the Mean-Variance associated to $U_{T_{(S)}}$ ($\overline{\sigma_{(S)}^2}$) and the Mean-Variance associated to $U_{T_{(SP)}}$ ($\overline{\sigma_{(SP)}^2}$) (Eq. (19)).

The steps carried out for the decoupling of the Temperature Uncertainty (U_T) are shown in the flowchart of Fig. 2 and are detailed in Ref. [17]:

1) The input data required to decouple the Temperature Uncertainty (U_T) are the Mean-Variances associated to the Temperature Uncertainty ($\overline{\sigma_T^2}$, Eq. (12) and Eq. (16)) and to the Temperature Sensor Uncertainty ($\overline{\sigma_{(S)}^2}$, Eq. (12) and Eq. (7)).
2) Then, the estimation of the Mean-Variance ($\overline{\sigma_{(SP)}^2}$) (Eq. (18)) and the Mean Standard Deviation ($\overline{\sigma_{(SP)}}$) associated with $U_{T_{(SP)}}$, can be obtained through Eq. (20) and Eq. (21) respectively, and thus, $U_{T_{(SP)}}$ can be estimated through Eq. (22).
3) Furthermore, the decoupling method allows us to know the relation between the Mean-Variance $\overline{\sigma_{(S)}^2}$ of the Temperature Sensor Uncertainty ($U_{T_{(S)}}$) concerning the Mean-Variance ($\overline{\sigma_T^2}$) of the Temperature Uncertainty (U_T). This relation is called, in this manuscript, the Sensor Ratio (R_S) and can be estimated through Eq. (23). This ratio represents the weight of the systematic causes over all uncertainties.
4) In the same way, the Spatial Ratio (R_{SP}) can be estimated through Eq. (24), which represents the weight of the random causes over all uncertainties.
5) Eq. (25) shows another way for the U_T estimation through $\overline{\sigma_{(S)}^2}$ and $\overline{\sigma_{(SP)}^2}$, taking into account their respective R_S and R_{SP} weights. A practical example of the R_S and R_{SP} estimation is shown in section 4.3 for each OT monitored in this study.
6) Finally, with a 95% confidence level, Eq. (26) shows the overall uncertainty range of the Volume Weighted Temperature ($\overline{T_{vw}}$) of a thermal zone for a studied period.

$$U_T = 2\left(\sqrt{\overline{\sigma_{(S)}^2} + \overline{\sigma_{(SP)}^2}}\right) = 2\left(\overline{\sigma_T}\right) = 2\left(\sqrt{\overline{\sigma_T^2}}\right) = 2\left(\sqrt{\frac{1}{N}\sum_{j=1}^{N}\sigma_{T_{\bar{t}_j}}^2}\right) = 2\left(\sqrt{\frac{1}{N}\sum_{j=1}^{N}\left[\sigma_{(S)t_j}^2 + \sigma_{(SP)t_j}^2\right]}\right) \quad [K \text{ or } ^\circ C] \tag{15}$$

$$\overline{\sigma_T^2} = \frac{1}{N}\sum_{j=1}^{N}\left[\sigma_{(S)t_j}^2 + \sigma_{(SP)t_j}^2\right] = \frac{1}{N}\left(\sigma_{(S)t_1}^2 + \sigma_{(S)t_2}^2 + \sigma_{(S)t_3}^2 + \ldots + \sigma_{(S)t_N}^2\right) + \frac{1}{N}\left(\sigma_{(SP)t_1}^2 + \sigma_{(SP)t_2}^2 + \sigma_{(SP)t_3}^2 + \ldots + \sigma_{(SP)t_N}^2\right) \quad [K^2] \tag{16}$$

$$\overline{\sigma_{(S)}^2} = \frac{1}{N}\left(\sigma_{(S)t_1}^2 + \sigma_{(S)t_2}^2 + \sigma_{(S)t_3}^2 + \ldots + \sigma_{(S)t_N}^2\right) \quad [K^2] \tag{17}$$

$$\overline{\sigma_{(SP)}^2} = \frac{1}{N}\left(\sigma_{(SP)t_1}^2 + \sigma_{(SP)t_2}^2 + \sigma_{(SP)t_3}^2 + \ldots + \sigma_{(SP)t_N}^2\right) \quad [K^2] \tag{18}$$

$$\overline{\sigma_T^2} = \overline{\sigma_{(S)}^2} + \overline{\sigma_{(SP)}^2} \quad [K^2] \tag{19}$$

$$\overline{\sigma_{(SP)}^2} = \overline{\sigma_T^2} - \overline{\sigma_{(S)}^2} \quad [K^2] \tag{20}$$

$$\overline{\sigma_{(SP)}} = \sqrt{\left(\overline{\sigma_T^2} - \overline{\sigma_{(S)}^2}\right)} \quad [K \text{ or } ^\circ C] \tag{21}$$

$$U_{T_{(SP)}} = 2\left(\overline{\sigma_{(SP)}}\right) \quad [K \text{ or } ^\circ C] \tag{22}$$

$$R_S = \frac{\overline{\sigma_{(S)}^2}}{\overline{\sigma_T^2}} \tag{23}$$

$$R_{SP} = \frac{\overline{\sigma_{(SP)}^2}}{\overline{\sigma_T^2}} = 1 - R_S \tag{24}$$

$$U_T = 2\left(\sqrt{\frac{\overline{\sigma_{(S)}^2}}{R_S}}\right) = 2\left(\sqrt{\frac{\overline{\sigma_{(SP)}^2}}{R_{SP}}}\right) \quad [K \text{ or } ^\circ C] \tag{25}$$

$$\overline{T_{vw}} - U_T \le \left(\overline{T_{vw}}\right)_{range} \le \overline{T_{vw}} + U_T \quad [K \text{ or } ^\circ C] \tag{26}$$

where,

U_T: Temperature Uncertainty [K or °C].
$\overline{\sigma_T^2}$: Mean-Variance of the sample [K^2].

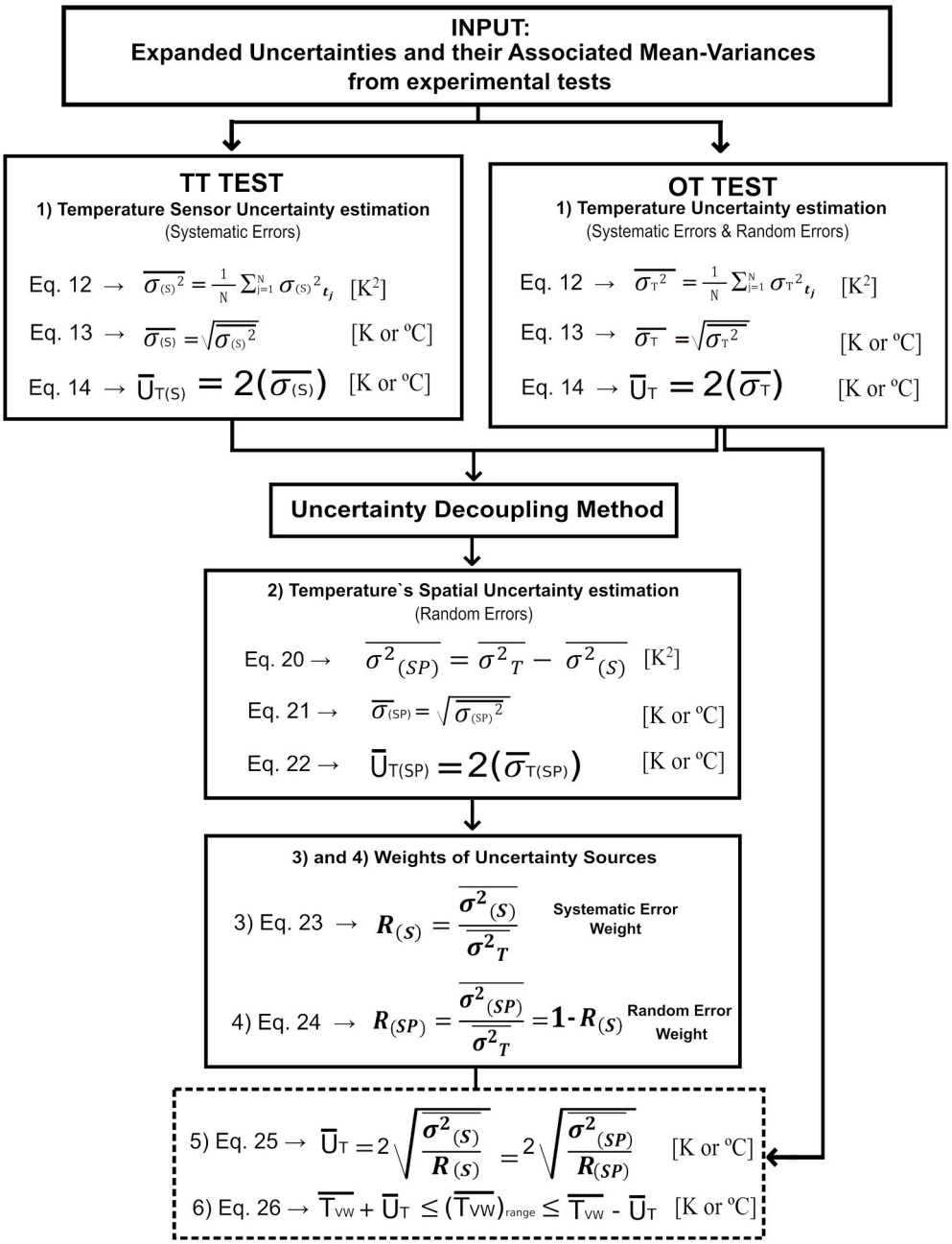

Fig. 2. Flowchart of the methodology to decouple the zonal indoor air Temperature Uncertainty (U_T) in the Temperature Sensor Uncertainty ($U_{T_{(S)}}$) and the Temperature's Spatial Uncertainty ($U_{T_{(SP)}}$).

$\overline{\sigma_T}$: Mean Standard Deviation of the sample, this value is associated with the overall Temperature Uncertainty estimation [K or °C].

$U_{T_{(SP)}}$: Temperature's Spatial Uncertainty [K or °C].

$\overline{\sigma^2_{(SP)}}$: Mean-Variance of the sample associated to $U_{T_{(SP)}}$ [K²].

$\overline{\sigma_{(SP)}}$: Mean Standard Deviation of the sample associated with the Temperature's Spatial Uncertainty ($U_{T_{(SP)}}$) [K or °C].

$U_{T_{(S)}}$: Temperature Sensor Uncertainty [K or °C].

$\overline{\sigma^2_{(S)}}$: Mean-Variance of the sample associated to $U_{T_{(S)}}$ [K²].

$\overline{\sigma_{(S)}}$: Mean Standard Deviation of the sample associated with the experimental Sensor Uncertainty ($U_{T(S)}$) [K or °C].

$\sigma^2_{T_{t_j}}$: Variance of Z Temperature Differentials θ_{dv_i} ($(\theta_{dv_i})_{vw}$ (Eq. (6)) or $(\theta_{dv_i})_a$ (Eq. (7)) for each t_j [K²].

$\sigma^2_{(S)t_j}$: Variance of Z Temperature Differentials θ_{dv_i} ($(\theta_{dv_i})_{vw}$ (Eq. (6)) or $(\theta_{dv_i})_a$ (Eq. (7)) for each t_j due to the Sensor Uncertainty ($U_{T(S)}$) [K²].

$\sigma^2_{(SP)t_j}$: Variance of Z Temperature Differentials θ_{dv_i} ($(\theta_{dv_i})_{vw}$ (Eq. (6)) or $(\theta_{dv_i})_a$ (Eq. (7)) for each t_j due to the Temperature's Spatial Uncertainty ($U_{T_{(SP)}}$) [K²].

R_{Sp}: Spatial Ratio, or Ratio of Mean-Variance, of the sample due to the Temperature's Spatial Uncertainty ($\overline{\sigma^2_{(SP)}}$) concerning the Mean-Variance of sample ($\overline{\sigma^2_T}$).

R_S: Sensor Ratio, or Ratio of the Mean-Variance, of the sample due to Sensor Uncertainty ($\overline{\sigma^2_{(S)}}$) concerning the Mean-Variance of the sample ($\overline{\sigma^2_T}$).

2.3. Thermal zone characterisation: Office typologies (OT)

The developed uncertainty estimation method is applicable to any thermal zone within a residential or tertiary building. However, to better understand and discuss the results of the zonal, T_{in} Uncertainties are estimated for the four monitored thermal zones presented in this research, and classification of those monitored Office Typologies (OT) has been done. An Office Typology is defined as a tertiary building thermal zone or volume composed of sub-volumes, which will be called Workspaces (WS). In the experimental test carried out [17], four-monitored OTs have been studied, consisting of different WS distributions, for which two types of WS were identified to characterise the OT:

- Open Workspace (OWS): This is a large space where there are many workstations without dividing walls.
- Compact Workspace (CWS): This is a space with less volume than the OWS, where there is one or a maximum of two workstations.

To characterise the OT, a relationship has been created based on the OWS volume and the number of CWS:

- Open Workspace Ratio (OWSR): This is the percentage of the volume occupied by open workspaces concerning the OT volume; this ratio is calculated according to Eq. (27).

$$OWSR = \frac{V_{OWS}}{V_{OT}} 100 \ [\%] \tag{27}$$

where,

V_{OWS}: Total open Workspace Volume within an OT [m^3].
V_{OT}: Total volume of an OT [m^3].

Six typologies have been defined in Table 5 to characterise the volume fraction occupied by the OWS.where,

N_{CWS} : Number of Compact Workspaces in an OT.
N_{OWS}: Number of Open Workspaces in an OT.

In Table 6, six typologies have been defined relative to the number of CWS.

3. Material

To test the proposed methodology, a Mobile Monitoring System (MMS) was designed and temporally installed in different OT of a tertiary building located in Leioa (Bilbao). This building had been retrofitted in 2018 as a demonstrator building of Affordable and Adaptable Public Buildings through the Energy Efficient Retrofitting (A2PBEER) project [21]. Since the air temperature of a volume is not homogenous, and to estimate the measurement uncertainties of the zonal indoor air temperature, several sensors had been installed in different places at different heights in the monitored thermal zones (OT in this case) of the building.

The MMS was installed in the building for interior monitoring and was conceived as a mobile system that can be adapted to different distances, heights and geometrics of each space so as to be able to change the MMS quickly to different areas and floors.

The MMS is composed of eight Tripods, twenty sensors (of which nineteen sensor measurements are used for the analysis developed in this manuscript), two gateways, Modbus wire and aerial connectors. The dataset analysed in this manuscript is available and explained in detail in the Data in Brief publication titled: "*Dataset of an in-use tertiary building collected from a detailed 3D Mobile Monitoring System and Building Automation System for indoor and outdoor air temperature analysis*" [22], which also explains the experimental test, including the methodology to conduct this research. In addition, the datasets are also available in a data repository [23]. This section will briefly outline part of the experimental test detailed in the mentioned Data in Brief ([17,22]) so as to facilitate the understanding of the results.

According to the typical practice to accomplish with the central limit theorem, the number for this analysis should be about 30 measurement points. However, based on physical knowledge about building physics, it is well known that stratification is one of the main sources of variability of the indoor air temperature within a thermal zone. This is the reason for choosing variable height tripods to locate the sensors within the analysed thermal zones. Thus, the position of the tripods has been as random as possible but always trying to cover the maximum area within each thermal zone, and very important, always preventing them from being exposed to direct solar radiation or affected by direct convective hot currents from the radiators. Since one of the main aims of this study was the overall uncertainty estimation of in-use thermal zones, the offices have been in-use during the tests, and the latter has imposed some restrictions for the position of the tripods.

Because of these issues, the number of measurement points for the selected thermal zones has been chosen to be 19 sensors. With this value, between 40 m^3 and 100 m^3 have been covered per sensor (note that the average volume of a European room is about 38 m^3 [24]). Actually, the presented methodology considers the instant of times as the sample, not the total number of temperature sensors. Thus, our analysis combines two dimensions: the total number of temperature sensors and the total number of time instants. Then, the analysis considers samples with thousands of time instants (with 19 temperature measurements per time instant); consequently, the sample size is orders of magnitude higher than 30. For example, the frequency distribution of the whole sample (including both dimensions, time instants and number of sensors) of OT4 can be seen in graphic (b) of Fig. 5. It can be clearly seen that considering only 19 measurement points; when combined with the dimension of the time, the analysed data series tends to a clear normal distribution. Therefore, although it cannot be ensured, it is not necessary to have 30 measurement points for this analysis; based on the knowledge of building physics and the normality check of the sample, it is considered to have sufficient sensors for this analysis.

Table 5
OWS typologies based on the OWSR.

- Division Factor (DF): This ratio defines the number of CWSs concerning the total number of WS in an OT, the sum of the number of OWSs and CWSs. This factor is calculated according to Eq. (28).

$$DF = \frac{N_{CWS}}{N_{CWS} + N_{OWS}} 100 \ [\%] \tag{28}$$

OWS Typologies	OWSR	Description
A	OWSR = 100%	Unique OWS
B	100 < OWSR <75%	Big volume of OWS
C	75% ≤ OWSR <50%	Medium volume of OWS
D	50% ≤ OWSR <25%	Small volume of OWS
E	25 ≤ OWSR <0%	Very small volume of OWS
F	OWSR = 0%	There is no OWS

Table 6
CWS Typologies based on DF.

CWS Typologies	DF	Description
6	DF = 100%	There is no OWS
5	100% < DF < 75%	Mainly CWS units
4	75% ≤ DF < 50%	Many CWS units
3	50% ≤ DF < 25%	Few CWS units
2	25% ≤ DF < 0%	Very few CWS units
1	DF = 0%	There is no CWS

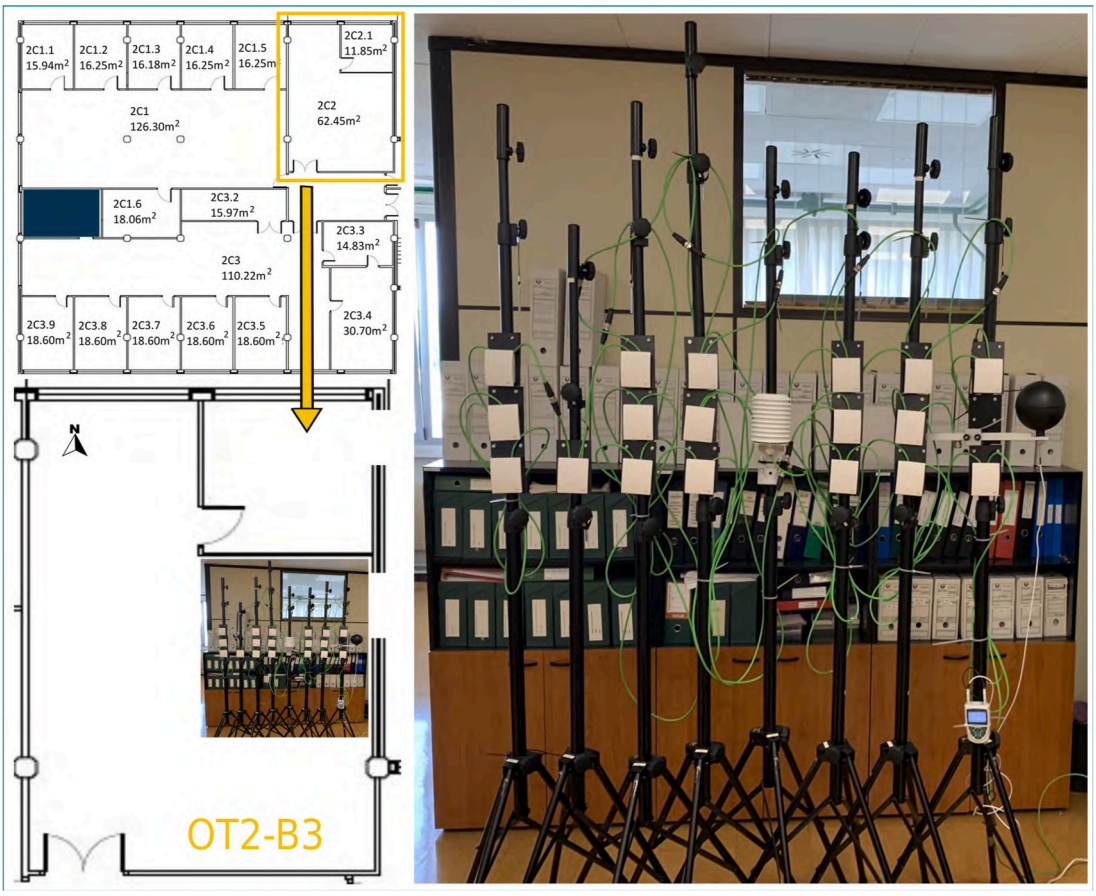

Fig. 3. EE800-M1213 and EE071-HTPC sensors located on the eight tripods during the Tripod Together (TT) test.

3.1. Monitored offices

The tertiary building studied is the west block of the University of the Basque Country (UPV/EHU) rectory; the building has four floors. A nursery is located on the ground floor (F0), and the other three floors are formed by work offices (floor one (F1), floor two (F2) and floor three (F3)).

Four thermal zones within the floors F2 and F3 of this tertiary building have been temporally monitored, which were selected because they represented four different distributions, each one representing an office typology. F2 has three independent OT (thermal zones) with different characteristics, while F3 has a unique OT. Their spatial distribution is shown in Appendix A, Fig. A1 and Fig. A2.

3.1.1. Office zone characterisation: office typologies (OT)

The Office Typologies monitored have the following characteristics, based on the number of workspaces:

- OT1: Located in F2. Represents an office with one OWS and six CWS.
- OT2: Located in F2. Represents an office with one OWS and one CWS.
- OT3: Located in F2. Represents an office with one OWS and eight CWS.
- OT4: Located in F3. Represents an office with one OWS and three CWS.

Based on the methodology shown in subsection 2.3, Table 8 shows the OWSR and DF values of each OT referred to in Table 2, Fig. A1 and Fig. A2. Likewise, in these figures, it is possible to identify the different OWS, CWS and the distribution of each thermal zone of F2 and F3.

3.2. The Mobile Monitoring System (MMS)

The criteria for the choice of technology in a Monitoring and Controlling System (MCS) are important to determine the accuracy level of the sensors and their measurements. The technology currently used on domotic systems and building automation systems does not have good precision and accuracy, so it is necessary to introduce technology with greater accuracy in order to increase the reliability of the MCS [25]. Based on this, the experimental test carried out was designed with criteria that guaranteed sensors with high accuracy and precision, which are described in detail in the Data in Brief publication [22]. The analysis carried out in this manuscript is based on the measurements of eighteen EE800-M12J3 sensors and one EE071-HTPC sensor (Table A1). Table A3 shows the sensor's location on each tripod, as well as the sensor and manufacturer's references.

Two experimental tests ([17,22]) were carried out to study the zonal indoor Air Temperature Uncertainty (U_T):

- Tripod Together (TT) test: All sensors were located at the same height and place to determine the experimental accuracy of the air temperature sensors installed within the MMS ($U_{T_{(S)}}$). Fig. 3 shows the TT test sensors measuring together. The TT Test was performed within the 2C2 volume of the OT2 during a "no use" period of this volume. This is a north-facing office; thus, there is no direct solar radiation entry on this volume. The test was performed at the end of June when there was no heating and, therefore, radiators are OFF and do not produce any convective currents. Performing the TT Test in-situ is crucial; this way, the Temperature Sensor Uncertainty ($U_{T(S)}$) is estimated with the same equipment with which the following temperature measurements of the thermal zones will be performed. The main assumption of this TT Test is that the volume

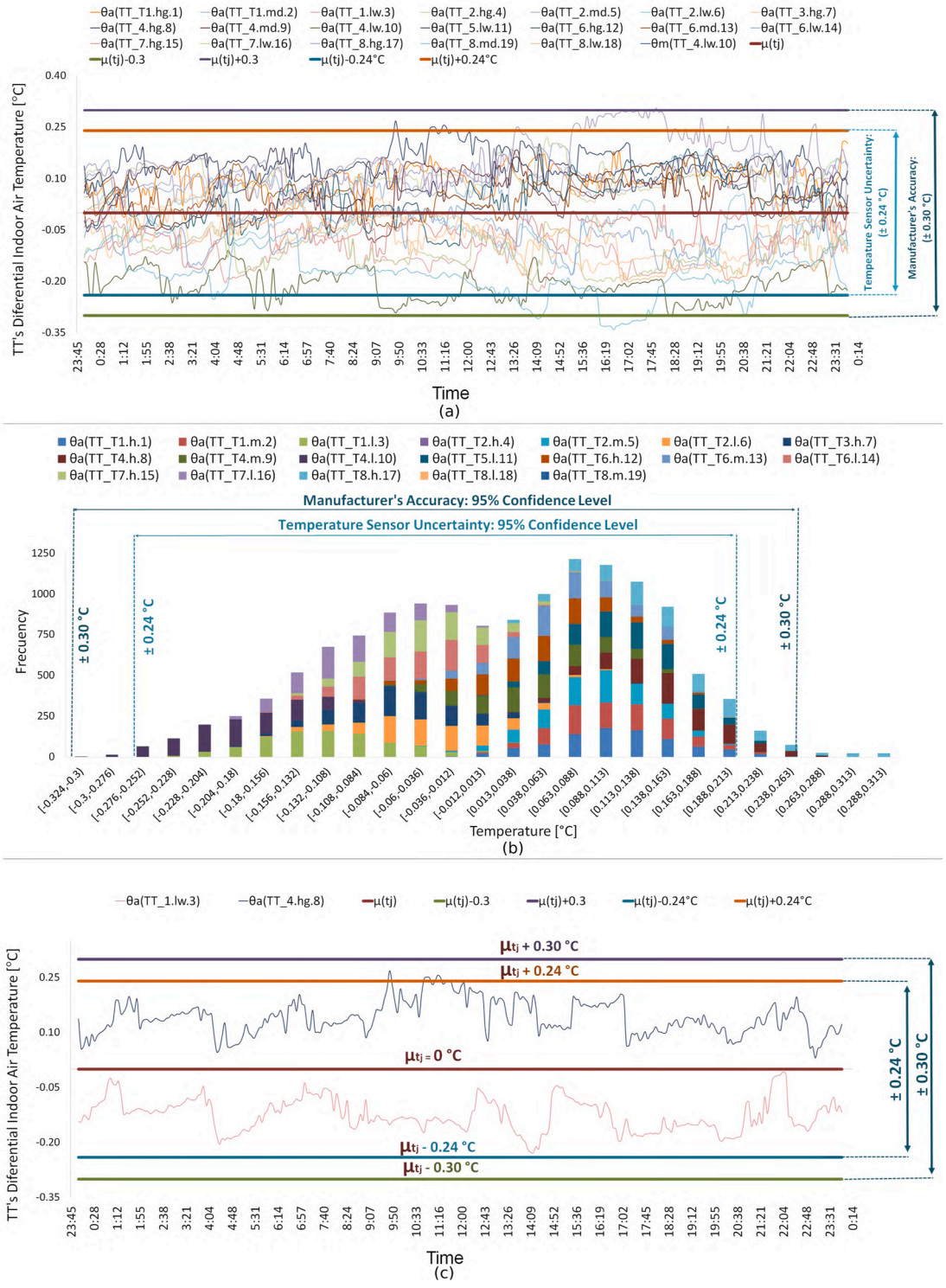

Fig. 4. (a): $(\theta_{dv_i})_a$ evolution of the 19 sensors during the TT test between 0:00 h and 24:00 h of June 30th, 2019. (b): histogram of all the $(\theta_{dv_i})_a$ values of the TT test, including the 95% confidence intervals of the experimental and manufacturer Temperature Sensor Uncertainty ($U_{T(S)}$). (c): detail of the evolution of the $(\theta_{dv_i})_a$ values of sensors TT_1.lw.3 and TT_4.hg.8, together with the evolution of the μ_{t_j} and the experimental and manufacturer Temperature Sensor Uncertainty ($U_{T(S)}$).

where all the sensors are located is so small that the temperature of such a small volume can be considered completely homogeneous in every instant of time.

- Office Typology (OT) tests: Eight tripods were located in the different WSs of each studied OT to determine their zonal indoor air Temperature Uncertainty (U_T). Table A2, Fig. A1 and Fig. A2 show the sensor layout of OT1, OT2, OT3 and OT4.

4. Results and discussion

The uncertainty analysis results of the zonal Indoor Air Temperature

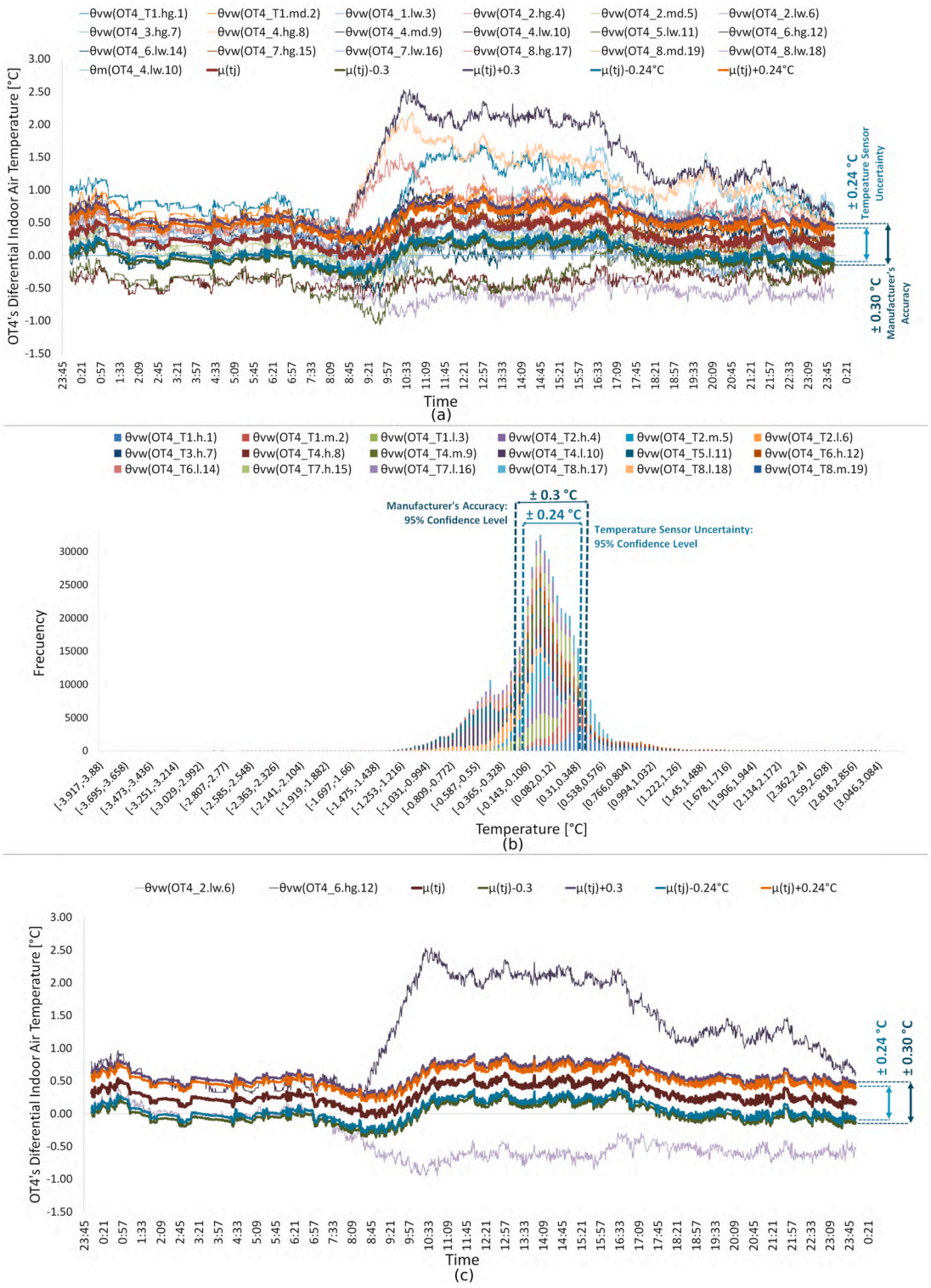

Fig. 5. (a): $(\theta_{dv_i})_{vw}$ evolution of the eighteen sensors during the OT4 test between 0:00 h and 24:00 h of April 24th, 2019. (b): histogram of all the $(\theta_{dv_i})_{vw}$ values of the OT4 test, including the 95% confidence intervals of the experimental and manufacturer Temperature Sensor Uncertainty ($U_{T(S)}$). (c): detail of the evolution of the $(\theta_{dv_i})_{vw}$ values of the sensors OT4_2.lw.6 and OT4_6.hg.12, together with the evolution of the μ_{t_j} and the experimental and manufacturer Temperature Sensor Uncertainty ($U_{T(S)}$).

in the four OTs presented above will be set out as follows:

- Temperature Sensor Uncertainty ($U_{T(S)}$) analysis.
- Temperature Uncertainty analysis (U_T) of each OT.
- Decoupling of Temperature Uncertainty (U_T) of each OT to estimate the Temperature's Spatial Uncertainty ($U_{T_{(SP)}}$).

4.1. Temperature Sensor Uncertainty ($U_{T(S)}$) analysis for the Mobile Monitoring System (MMS)

This study provides insights into the experimental measurement accuracy for the sensor technology installed in the MMS. In this experimental test, all the sensors were left together at the same height (at a

Table 7
Statistical results of Temperature Sensor Uncertainty ($U_{T(S)}$) analysis for the Mobile Monitoring System (MMS).

Statistical Analysis	Nineteen sensor	Eighteen sensors[a]	Units
Sample Size (N)	868	868	–
Global Mean ($\bar{\mu}$) (Eq. (11))	0.00	0.00	[°C]
Mean Variance ($\overline{\sigma^2_{(S)}}$) (Eq. (12))	**0.014**	**0.013**	[K^2]
Mean Standard Deviation https://elsevier.proofcentral.com/en-us/landing-page.html?token=19bee0fe660792b7050a6a6fea63bb**($\overline{\sigma_{(S)}}$) (Eq. (13))**	**0.119**	**0.113**	[°C]
Expanded Uncertainty ($U_{T(S)}$) (Eq. (14))	**±0.24**	**±0.22**	[°C]
Min	−0.44	−0.33	[°C]
Max	0.31	0.29	[°C]

[a] Excluding the EE071-HTPC sensor measurement.

Table 8
Analysed thermal zones (OT in this case) classification.

Office Reference	CWS Number	OWSR (Eq. (27))	DF (Eq. (28))	OWS-CWS Typology	Office Typology Name
OT1	6	**58.10%**	**85.71%**	C-5	**OT1-C5**
OT2	1	**84.18%**	**50.00%**	B-3	**OT2-B3**
OT3	8	**41.59%**	**88.89%**	D-5	**OT3-D5**
OT4	3	**87.26%**	**75.00%**	B-4	**OT4-B4**

medium level of 174 cm with a strip of ±12 cm, see Fig. 3), measuring from June 28th, 2019, at 11:55 a.m. to July 01st, 2019 at 12:10 p.m. Fig. A3 shows the evolution of all T_{dv_i} during 24 h of data collected from the TT test ([22,23]) on June 30th, 2019, from 0:00 to 24:00. Table 7 shows the statistical analysis results for a sample size of N = 868, each t_j with nineteen-temperature measurements collected at a measurement frequency of 5 min.

According to the methodology described in subsections 2.2.1 and 2.2.2, Eq. (13) provides a $\overline{\sigma_{(S)}}$ value of 0.119 °C, then (Eq. (14)) provides a $U_{T(S)}$ value of ±0.24 °C for the MMS. The $U_{T(S)}$ value is less than the accuracy of the EE800-M1213 sensor, based on the manufacturer's values shown in Table A1Table A1, which is ±0.30 °C, with both values differing by 20% from the manufacturer's accuracy.

These statistical parameters considering only eighteen sensors, excluding the EE071-HTPC sensor, provide a $U_{T(S)}$ value of ±0.22 °C; with the MMS being more accurate using only EE800-M1213 sensors, and the $\overline{\sigma_{(S)}}$ value being 0.113 °C, which is 0.006 °C less than the $\overline{\sigma_{(S)}}$ value obtained from the statistical analysis of the nineteen sensors. The $U_{T(S)}$ value for the MMS in the following estimates in this manuscript will be ±0.24 °C, which considers the systematic errors of both sensor technologies used (EE800-M1213 and EE071-HTPC) plus the MMS.

Fig. 4 shows the evolution (graphic a) and the histogram (graphic b) of the analysed $(\theta_{dv_i})_a$ values. Likewise, the manufacturer's sensor accuracy values and the estimated ($U_{T(S)}$) of the sensors plus MMS are also plotted. The graph shows how, in the test carried out, by installing the sensors in close proximity to each other, temperature measurements can be obtained, which only include uncertainties associated with systematic errors. In the histogram plot, it has been calculated that the 99.60% of data are within the manufacturer's accuracy range (±0.30 °C), and when the estimated ($U_{T(S)}$) is taken into account, 97.83% of data lie within ±0.24 °C. In case of a perfect normal distribution, 95% of the data would be within the ±0.24 °C range of Fig. 4 (b). Thus, this is another sign of the correctness of the normality assumption considered in this work for the analysed $(\theta_{dv_i})_a$ values. Finally, for clarity, in Fig. 4 (c), a detail of the evolution of the $(\theta_{dv_i})_a$ values of sensors TT_1.lw.3 and TT_4.hg.8, together with the evolution of the μ_{t_j} and the experimental and manufacturer Temperature Sensor Uncertainty ($U_{T(S)}$) is shown.

4.2. Zonal indoor air temperature uncertainty (U_T) analysis of the four-studied OTs

The methodology applied to analyse the U_T for the four OTs is described in subsections 2.2.1 and 2.2.3. The estimated U_T value includes all sources of uncertainty that have an impact on the zonal indoor air temperature measurement of the considered thermal zone, the random errors (Temperature's Spatial Uncertainty ($U_{T(SP)}$) and the systematic errors (Temperature Sensor Uncertainty ($U_{T(S)}$)).

Fig. A1 and Fig. A2 allow us to identify the interior and exterior CWSs facing north, south, west and those with multiple cardinal orientations. Furthermore, as an illustrative example, Fig. A4 shows in detail a 24-h sample of the T_{dv_i} evolution of data collected for OT4 test, ([22,23]).

The OT tests were carried out in the following periods:

- OT1: From June 06, 2019, at 14:11:40 to June 23, 2019, at 05:29:10, every 10 s.
- OT2: From June 06, 2019, at 14:20:50 to June 23, 2019, at 05:07:30, every 10 s.
- OT3: From May 19, 2019 at 7:09:10 to May 30, 2019, at 5:05:50, every 50 s.
- OT4: From April 12, 2019 at 14:43:20 to April 29, 2019, at 00:06:40, every 40 s.

Table 8 shows the office zone's classification results for the OWSR and DF values based on the methodology described in subsection 2.3: the OWS-CWS typology of office one is C5 (named OT1-C5); of office two, it is B3 (called OT2-B3); of office three, it is D5 (named OT3-D5); and of office four, it is B4 (named OT4-B4). OT1-C5, facing north-west, has six CWSs and OT3-D5, while facing south-west, it has eight CWSs; both OTs have similar OWSR and identical DF typology. Both these OTs have many CWSs, and an OWS occupies nearly 50% of the volume. The OT2-B3, oriented to the north, has one CWS, and 84.18% of the volume is occupied by an OWS. In addition, OT4-B4, facing north-south-west, has three CWSs and a similar OWSR to OT2-B3. This OT has the same OWS typology but a total volume considerably greater than OT2-B3.

For each analysed OT, Table 9 shows the statistical results of the $(\theta_{dv_i})_{vw}$ values calculated with (Eq. (6)). OT1-C5, with fourteen temperature sensors, has its $\overline{\sigma^2_T}$, $\overline{\sigma_T}$ and U_T values equal to 0.127 K^2, 0.356 °C and ±0.71 °C, respectively. OT2-B3, with five temperature sensors, has $\overline{\sigma^2_T}$, $\overline{\sigma_T}$ and U_T values equal to 0.135 K^2, 0.368 °C and ±0.74 °C, respectively. OT3-D5, with nineteen temperature sensors, has $\overline{\sigma^2_T}$, $\overline{\sigma_T}$ and U_T values equal to 0.287 K^2, 0.536 °C and ±1.07 °C, respectively. In addition, OT4-B4, with eighteen temperature sensors, has $\overline{\sigma^2_T}$, $\overline{\sigma_T}$ and U_T values equal to 0.172 K^2, 0.414 °C and ±0.83 °C, respectively.

OT1-C5 and OT2-B3 have an almost equal uncertainty value and the

Table 9
Sample statistical results and zonal indoor overall Temperature Uncertainty (U_T) estimation for each OT.

Office Typology	CWS Number	Sample Size (N)	Measure Numbers (p) by t_j	Global Mean ($\overline{\mu}$)[a] [°C] (Eq. (11))	Mean Variance ($\overline{\sigma_T^2}$)[a] [K^2] (Eq. (12))	Mean Standard Deviation ($\overline{\sigma_T}$)[a] [°C] (Eq. (13))	Temperature Uncertainty (U_T)[a] [°C] (Eq. (14), Eq. (15))
OT1-C5	6	28,733	14	0.144	0.127	0.356	**±0.71**
OT2-B3	1	28,705	5	−0.174	0.135	0.368	**±0.74**
OT3-D5	8	18,861	19	−0.033	0.287	0.536	**±1.07**
OT4-B4	3	35,381	18	−0.031	0.172	0.414	**±0.83**

[a] Values calculated based on the methodology described in section 2.2 and sub-section 2.2.3.

lowest value of the four studied OT; both have the main façade oriented to the north, a very different OWS-CWS typology (Table 8), and a different number of sensors to measure the indoor air temperature. OT4-B4 has a slightly higher U_T value with respect to OT1-C5 and OT2-B3; this OT has the same OWSR (Table 8) as OT2-B3 but is different from OT1-C5. What these three OTs have in common is that they have one main façade oriented to the north. Finally, OT3-D5 has the highest U_T value; this OT has a different typology from the others and does not have a north-facing facade, while its main façade faces south.

Comparing these overall uncertainty results (U_T) with the manufacturer's sensor accuracy (Table A1)Table A1, the U_T values of each OT are 2.4–3.6 times higher than the ±0.30 °C manufacturer's sensor accuracy stated for EE800-M12J3, or 7 to 10.7 times higher than the ±0.10 °C manufacturer's sensor accuracy stated for the EE071-HTPC. Note that these same sensors during the TT Test had an overall uncertainty of ±0.24 °C; thus, the temperature variability within the analysed four OT (or thermal zones) produced a considerable uncertainty in the representative temperature of the analysed OTs.

4.3. *Temperature uncertainty (U_T) decoupling analysis to estimate Temperature's Spatial Uncertainty ($U_{T_{(SP)}}$)*

Section 2.2.4 set out the methodology for decoupling U_T to estimate the Temperature's Spatial Uncertainty $U_{T_{(SP)}}$ value from the already estimated $U_{T(S)}$ and U_T values. The $U_{T(S)}$ value is ±0.24 °C (estimated in section 4.1) and the U_T values for the studied thermal zones (OT) are estimated in section 4.2, whose values are shown in Table 9.

Table 10 shows the results of the R_{SP}, R_S and $U_{T_{(SP)}}$ values by means of the application of the overall uncertainty decoupling method detailed in section 2.2.4. The R_{SP} values in the OTs are 88.86%, 89.57%, 95.09% and 91.77% for OT1-C5, OT2-B3, OT3-D5 and OT4-B4, respectively. These values show that within the U_T values, random errors have a greater weight than systematic errors. Likewise, R_S in all the OTs show that the systematic errors have low impact on the zonal T_{in} measurement uncertainty, being equal to 11.14%, 10.43%, 4.91%, and 8.23% for OT1-C5, OT2-B3, OT3-D5 and OT4-B4, respectively. Finally, the $U_{T_{(SP)}}$ values are congruent with the R_{SP} values, being equal to ±0.67 °C, ±0.70 °C, ±1.05 °C and ±0.79 °C for OT1-C5, OT2-B3, OT3-D5 and OT4-B4, respectively. Where OT3-D5 has the highest uncertainty due to random errors and OT1-C5 the lowest $U_{T_{(SP)}}$ value .

These results are logical since OT3-D5 is the thermal zone with the highest south façade area regarding its total volume. Thus, the OT3-D5 is the most exposed to direct solar radiation effects, which means that the temperature measurements have greater spatial variability due to the randomness derived from this solar exposure. In addition, within OT3-D5, six WS are highly exposed to direct solar radiation, one is slightly exposed (2C3), and two are not exposed (2C3.2 and 2C3.3). This is another reason for having more significant spatial variability on the temperature within this OT3-D5 volume and consequently a higher uncertainty on the OT3-D5 thermal zone indoor air temperature. The OT1-C5 is just the opposite case regarding direct solar radiation exposure. The façade area of thermal zone OT1-C5 is mainly oriented to the north, so its main envelope is not exposed to direct solar radiation. Thus, solar radiation does not produce a spatial temperature variability within this thermal zone, reducing the random uncertainties associated with direct exposure to solar radiation.

Fig. 5 ((a), (b) and (c)) graphically show how random errors can affect the T_{in} measurement, where most of the $(\theta_{dv_i})_{vw}$ signals in the OT4 test deviate considerably from the $U_{T(S)}$ range estimated for the MMS and the manufacturer's sensor accuracy. As an example, in this Figure, graphic (c) shows a zoom of the OT4_2.lw.6 and OT4_6.hg12 $(\theta_{dv_i})_{vw}$ signals, where the random errors effect is best appreciated. Likewise, the plotted histogram (graphic (b)) shows how the $(\theta_{dv_i})_{vw}$ data set tends to a normal distribution, and a large amount of the $(\theta_{dv_i})_{vw}$ data is outside the $U_{T(S)}$ range estimated for the sensor plus MMS (±0.24 °C) and outside the manufacturer's accuracy (±0.30 °C).

Finally, Table 11 shows the volume-weighted zonal indoor air temperature in each analysed OTs averaged for the whole monitoring

Table 11
Volume weighted average zonal indoor air temperature for each OT.

Office Typology	Monitoring Period Averaged Volume Weighted Temperature ($(\overline{T_{vw}})_{OT}$) [°C] (Eq. (5))	Expanded Uncertainty (U_T)[°C] (Eq. (14))	95% Confidence Range Low Limit [°C] (Eq. (26))	95% Confidence Range High Limit [°C] (Eq. (26))
OT1-C5	22.83	±0.71	**22.12**	**23.55**
OT2-B3	22.57	±0.74	**21.83**	**23.30**
OT3-D5	23.33	±1.07	**22.25**	**24.40**
OT4-B4	22.99	±0.83	**22.17**	**23.82**

Table 10
Decoupling the Mean Standard Deviation of each sample and the R_{SP}, R_S and $U_{T_{(SP)}}$ estimation for each OT.

Values from $U_{T(S)}$ Analysis (Table 7): $\overline{\sigma^2_{(S)}}$ = 0.014 K^2, $\overline{\sigma}_{(S)}$ = 0.119 °C, $U_{T(S)}$ = ±0.24 °C

Office Typology	$\overline{\sigma^2_{(S)}}$ (Eq. (12)) [K^2]	$\overline{\sigma^2_T}$ (Eq. (12)) [K^2]	$\overline{\sigma^2_{(SP)}}$ (Eq. (20)) [K^2]	$\overline{\sigma}_{(SP)}$ (Eq. (21)) [°C]	$U_{T_{(SP)}}$ (Eq. (22)) [°C]	R_S (Eq. (23))	R_{SP} (Eq. (24))
OT1-C5	0.014	0.127	0.113	**0.335**	**±0.67**	**11.14%**	**88.86%**
OT2-B3	0.014	0.135	0.121	**0.348**	**±0.70**	**10.43%**	**89.57%**
OT3-D5	0.014	0.287	0.273	**0.523**	**±1.05**	**4.91%**	**95.09%**
OT4-B4	0.014	0.172	0.157	**0.397**	**±0.79**	**8.23%**	**91.77%**

period. This Table also shows, with a 95% confidence, the overall uncertainty of those zonal indoor air temperatures for each OT.

5. Conclusions

In this research, high-quality indoor air temperature measurements of different thermal zones of an in-use office building have been statistically analysed to evaluate different zonal indoor air temperature measurement uncertainty components. The main conclusion is that the overall temperature uncertainty of the monitored thermal zones is 2.4–10.7 times bigger than the manufacturer's accuracy for sensors. Thus, using the manufacturer's accuracy as the overall temperature uncertainty value for the indoor air temperature measurement of a thermal zone could greatly underestimate the uncertainty of a thermal zone temperature.

This paper has presented the development of a method that permits monitored indoor air temperature measurements to be analysed to estimate both the overall temperature uncertainty of a thermal zone and the uncertainty associated with the systematic error of the temperature sensors (including the uncertainty related to the monitoring system where sensors have been installed). Furthermore, through the decoupling method developed in this study, it is analytically possible to estimate the uncertainty associated with the random errors of temperature measurements of a thermal zone.

The results of the first study to estimate the experimental accuracy by estimating the Temperature Sensor Uncertainty show that there is even a discrepancy between the sensor accuracy given by the manufacturer and the experimental accuracy of the sensor plus the monitoring equipment. In the studied case, the manufacturer's accuracy for the sensors used was ± 0.30 °C and ± 0.10 °C. In contrast, the uncertainty associated with the used temperature sensor technology plus the uncertainty related to the monitoring system has been estimated to be ± 0.24 °C.

Once the Temperature Sensor Uncertainty had been estimated in the first study, the overall uncertainty estimation and its decoupling were carried out. The classification of office typologies has been developed to better understand and analyse the uncertainty analysis results. Based on this Office Typology classification, four thermal zones with different geometric and spatial characteristics were selected for monitoring in an in-use office building. The following overall zonal indoor air temperature uncertainty values were obtained after applying the developed statistical method: ± 0.71 °C, ± 0.74 °C, ± 1.07 °C and ± 0.83 °C. The offices with a larger south-facing façade area have greater Temperature Uncertainty than the offices with a larger north-facing façade area. The thermal zones (offices in this case) with large south and north-facing façade areas have uncertainty values close to the offices with only one large north-facing façade area. During this study, two different types of sensors have been used, eighteen with a 0.30 °C manufacturer's accuracy and one with a 0.10 °C manufacturer's accuracy. So, it can be seen that the overall uncertainties calculated, with a 95% confidence interval, are 2.4–3.6 times higher than the ± 0.30 °C manufacturer's sensor accuracy, or 7 to 10.7 times higher than the ± 0.10 °C manufacturer's sensor accuracy.

Finally, based on a proposed decoupling method, the estimated overall temperature uncertainties were decoupled using the already estimated sensor plus monitoring system uncertainty to obtain the Temperature's Spatial Uncertainty, where all the other sources of uncertainty, excluding the sensor plus monitoring system, are considered. To estimate the weight of the different sources of uncertainty, the Ratio of the Mean-Variance due to the Sensor Uncertainty over the Mean-Variance due to the overall Temperature Uncertainty has been defined as R_S. This ratio has allowed us to know the percentage weight of the sensor plus monitoring system uncertainty over the overall temperature uncertainty for the four studied Office Typologies. In the case of the said Office Typologies, the weight has values between 5% and 11%. In addition, the Ratio of the Mean-Variance due to the Spatial Temperature Uncertainty (R_{SP}) has been defined in an analogous way, and the obtained values range between 89% and 95%. Both ratio values, R_S and R_{SP}, allow us to know the degree of importance of all the Spatial Uncertainties, $U_{T(SP)}$, excluding the uncertainty associated with the sensors plus monitoring system, over thermal zones where the temperature measurements have been performed.

With these estimated overall Temperature Uncertainty values, it will be possible to study the propagation of the zonal indoor air temperature overall uncertainty in different fields where the thermal zones' indoor air temperature is used for calculation purposes of in-use buildings.

In further research, future studies could be carried out on the estimated Temperature's Spatial Uncertainty to discover the individual effects of the ON/OFF of the solar radiation, the heating system, the ventilation system, and the electricity consumption among others. Furthermore, the study of the best location and number of sensors to estimate the zonal indoor air temperature measurement uncertainty in in-use buildings' thermal zones could be performed. In addition, the study of how the overall uncertainty estimation varies depending on the season would be of great interest.

CRediT authorship contribution statement

Catalina Giraldo-Soto: Writing – original draft, Visualization, Validation, Software, Resources, Methodology, Investigation, Formal analysis, Data curation, Conceptualization. **Laurent Mora:** Writing – review & editing, Validation, Supervision, Resources, Project administration, Methodology, Conceptualization. **Aitor Erkoreka:** Writing – review & editing, Validation, Supervision, Resources, Project administration, Funding acquisition, Conceptualization. **Irati Uriarte:** Writing – review & editing, Resources. **Pablo Eguia:** Writing – review & editing, Validation, Funding acquisition.

Declaration of competing interest

The authors declare that they have no known competing financial interests or personal relationships that could have appeared to influence the work reported in this paper.

Acknowledgements

This work was supported by the Spanish Ministry of Science, Innovation and Universities and the European Regional Development Fund through the project called 'Investigation of monitoring techniques of occupied buildings for their thermal characterisation and methodology to identify their key performance indicators', project reference: RTI2018-096296-B-C22 and - C21 (MCIU/AEI/FEDER, UE).

The corresponding author also acknowledges the support provided by the University of the Basque Country and the University of Bordeaux through a scholarship granted to Dr Catalina Giraldo-Soto to complete her PhD degree through the Framework Agreement: Euro-regional Campus of Excellence within the context of their respective excellence projects, Euskampus and IdEx Bordeaux. Funder reference: PIFBUR 16/26.University of the Basque Country (UPV/EHU).

Appendix A

Table A1
Technical characteristics of sensors and gateway of the MMS.

SENSORS			
Reference	Producer	Measure	Accuracy
EE800-M12J3 [26]	E + E Electronik	Temperature	±0.3 °C
		Relative Humidity	±3% RH(30.70%RH) ±5% RH(10.90%RH)
		Carbon Dioxide	0 … 2000 ppm < ± (50 ppm + 2% of measuring value)
EE071-HTPC [27]		Temperature	±0.1 °C at 23 °C
		Relative Humidity	±2% RH (0 … 90% RH) ±3% RH (0 … 100% RH)
GATEWAY			
Reference	**Producer**	**Protocols**	**Technical Characteristics**
KNXRTU1K [28]	DEEI	KNX to Modbus RTU-RS485	RS485 Half-Duplex interface for Modbus RTU. The 120-Ω RS485 termination resistor inside the gateway. Operating temperature −40 to +85 °C. Maximum number of points 1000. Supports Boolean data, 8 bits, 16 bits, 32 bits, 64 bits, float 16, float 32.

Table A2
Geometric characteristics of the studied thermal zones. Based on [17,22].

Office Reference	Cardinal Orientation of OT's Façade	WS References	WS Type	WS Orientation***	Area (m^2)**	Height (m)**	Volume (m^3)**
OT1	North, West	2C1	OWS	West	126.03	3.39	427.24
OT1	North, West	2C1.1	CWS	West-North	15.94	3.07	48.94
OT1	North, West	2C1.2	CWS	North	16.25	3.10	50.38
OT1	North, West	2C1.3	CWS	North	16.18	3.11	50.32
OT1	North, West	2C1.4	CWS	North	16.25	3.12	50.62
OT1	North, West	2C1.5	CWS	North	16.25	3.13	50.86
OT1	North, West	2C1.6	CWS	Interior	18.06	3.16	56.98
OT2	North	2C2	OWS	North	62.45	3.15	196.72
OT2	North	2C2.1	CWS	North	11.85	3.12	36.97
OT3	South, West	2C3	OWS	South-West	110.22	2.95	325.15
OT3	South, West	2C3.2	CWS	Interior	15.97	3.13	49.99
OT3	South, West	2C3.3	CWS	Interior	14.83	2.91	43.08
OT3	South, West	2C3.4	CWS	South	30.70	2.98	91.49
OT3	South, West	2C3.5	CWS	South	18.60	2.98	55.34
OT3	South, West	2C3.6	CWS	South	18.60	2.95	54.87
OT3	South, West	2C3.7	CWS	South	18.53	2.93	54.29
OT3	South, West	2C3.8	CWS	South	18.60	2.93	54.41
OT3	South, West	2C3.9	CWS	South-West	18.21	2.93	53.26
OT4*	South, West, North	3C1	OWS	South-West-North	400.40	3.55	1472.98
OT4*	South, West, North	3C1.1	CWS	North	16.10	3.36	54.02
OT4*	South, West, North	3C1.2	CWS	South-West	23.99	3.36	80.49
OT4*	South, West, North	3C1.3	CWS	West-North	23.99	3.36	80.49

* The 3C1 height showed is a mean value as there are different heights; nevertheless, the volume shown takes into account the different heights of this WS.
** Values shown in Fig. A1 and Fig. A2.
*** It only indicates the cardinal orientation of the sides of the WS facing the exterior facade.

Table A3
Sensor references installed on the eight tripods and tripod level location. Based on [17,22].

Sensor Reference	Tripod Number	Height*	Sensor Manufacture Reference
T1.hg.1	T1	hg	EE800-M12J3
T1.md.2	T1	md	EE800-M12J3
T1.lw.3	T1	lw	EE800-M12J3
T2.hg.4	T2	hg	EE800-M12J3
T2.md.5	T2	md	EE800-M12J3
T2.lw.6	T2	lw	EE800-M12J3
T3.hg.7	T3	hg	EE800-M12J3
T4.hg.8	T4	hg	EE800-M12J3
T4.md.9	T4	md	EE800-M12J3
T4.lw.10	T4	lw	EE800-M12J3
T5.lw.11	T5	lw	EE800-M12J3
T6.hg.12	T6	hg	EE800-M12J3
T6.md.13	T6	md	EE800-M12J3
T6.lw.14	T6	lw	EE800-M12J3

(*continued on next page*)

Table A3 (*continued*)

Sensor Reference	Tripod Number	Height*	Sensor Manufacture Reference
T7.hg.15	T7	hg	EE800-M12J3
T7.lw.16	T7	lw	EE800-M12J3
T8.hg.17	T8	lw	EE800-M12J3
T8.md.19	T8	hg	EE071-HTPC**
T8.lw.18	T8	md	EE800-M12J3

* Height: High (hg), medium (md) and low (lw).
** EE071-HTP protected within a radiation shielding without mechanical ventilation.

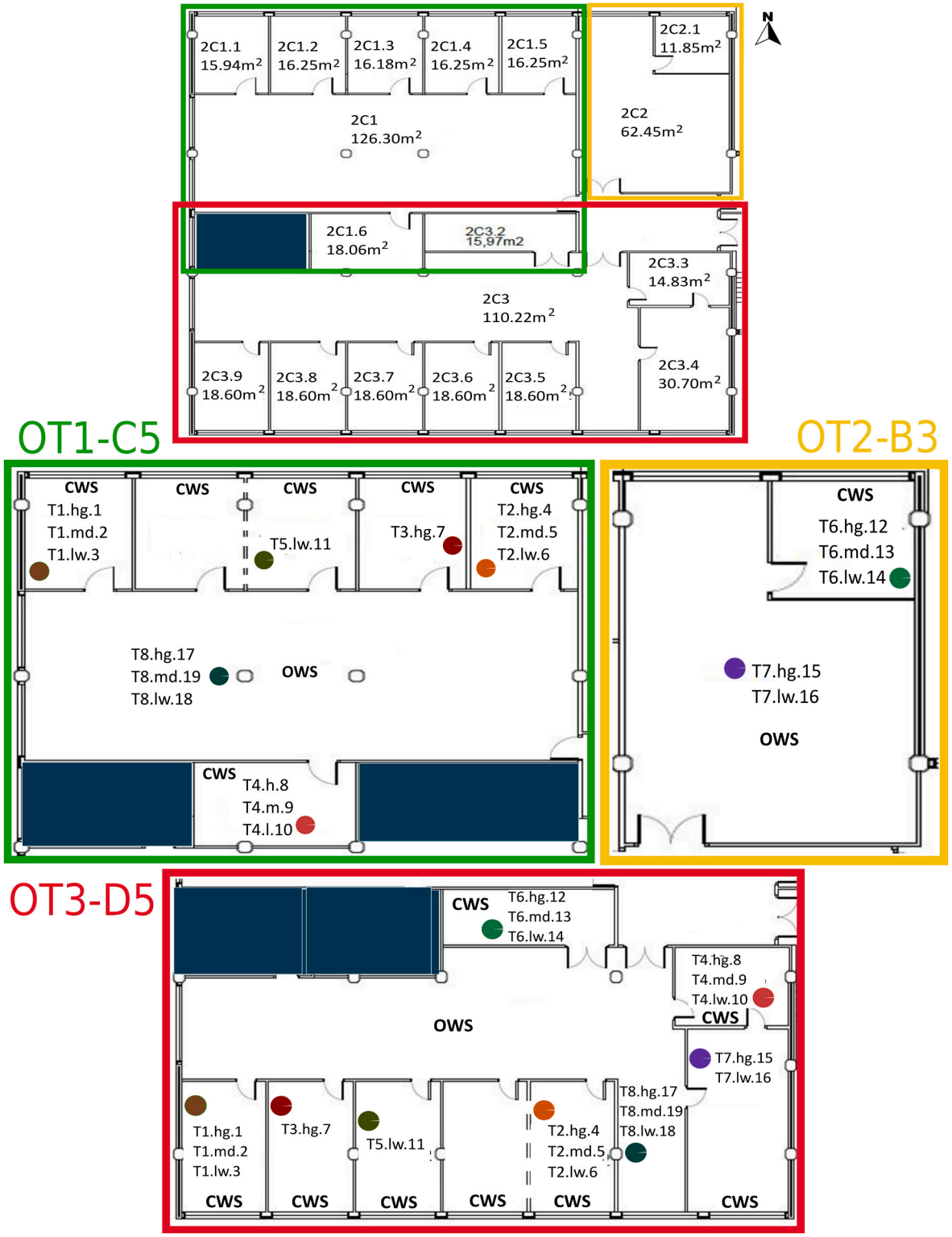

Fig. A1. OT1, OT2 and OT3 distribution, located in F2, see also [22].

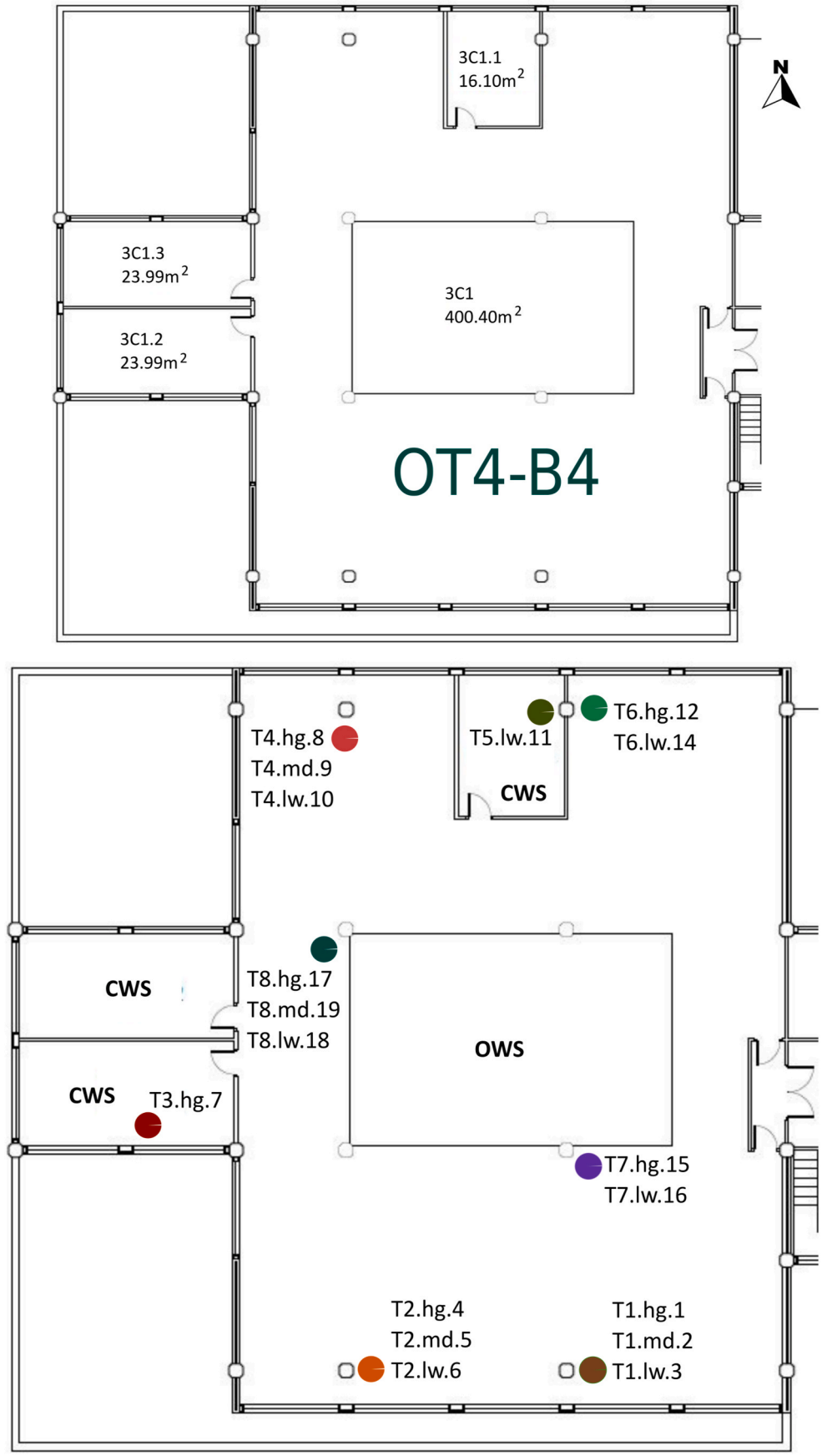

Fig. A2. OT4 distribution, located in F3, see also [22].

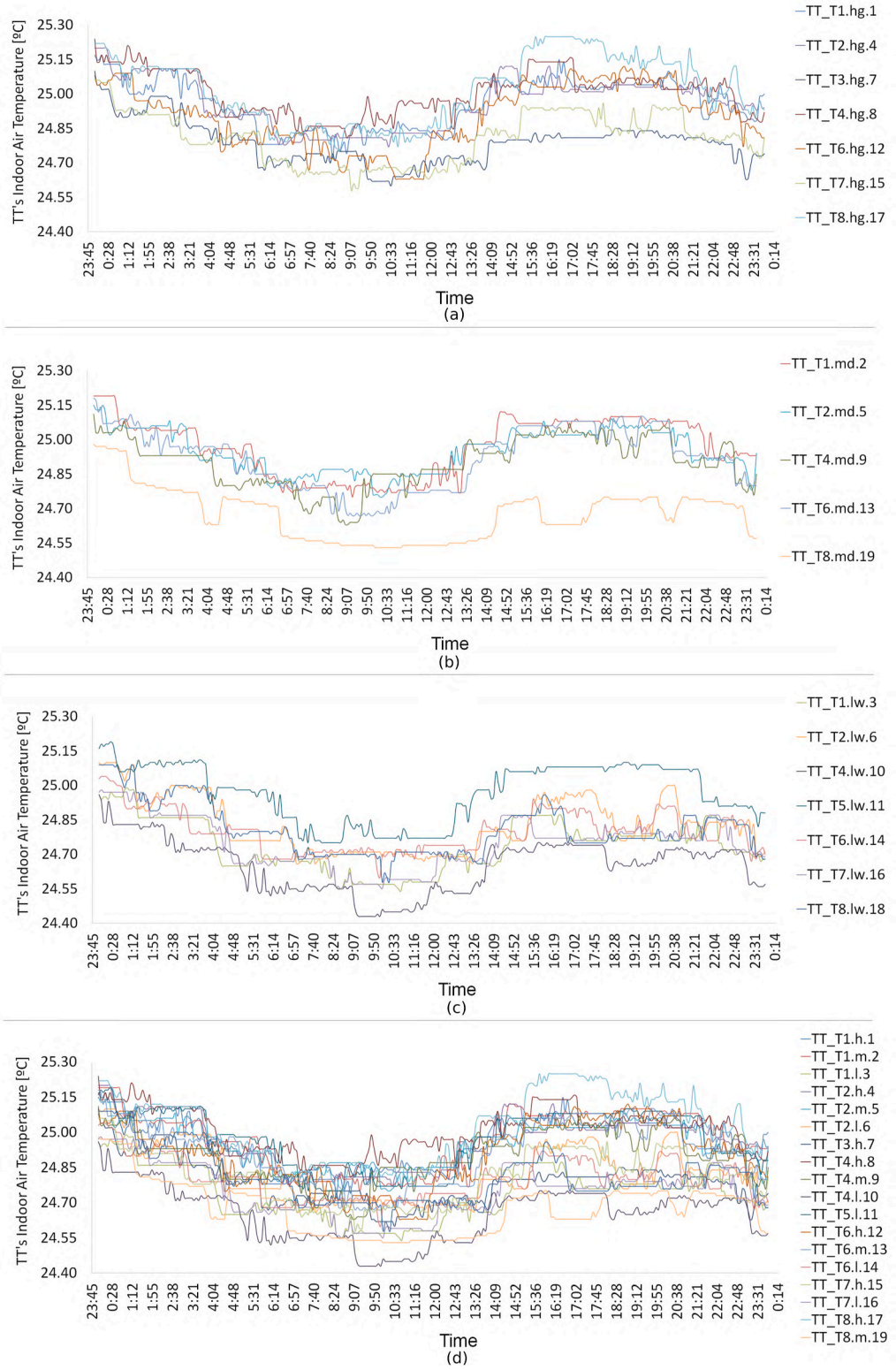

Fig. A3. Details of T_{dv_i} evolution in 24 h of data collected from the TT test between June 30th, 2019 at 0:00 to 24:00. (TT test ([22,23])). First three Figures shows the temperature measurements grouped by height location of the sensor on the tripods: (a) high height, (b) middle height and (c) low height. Figure (d) shows all signals together.

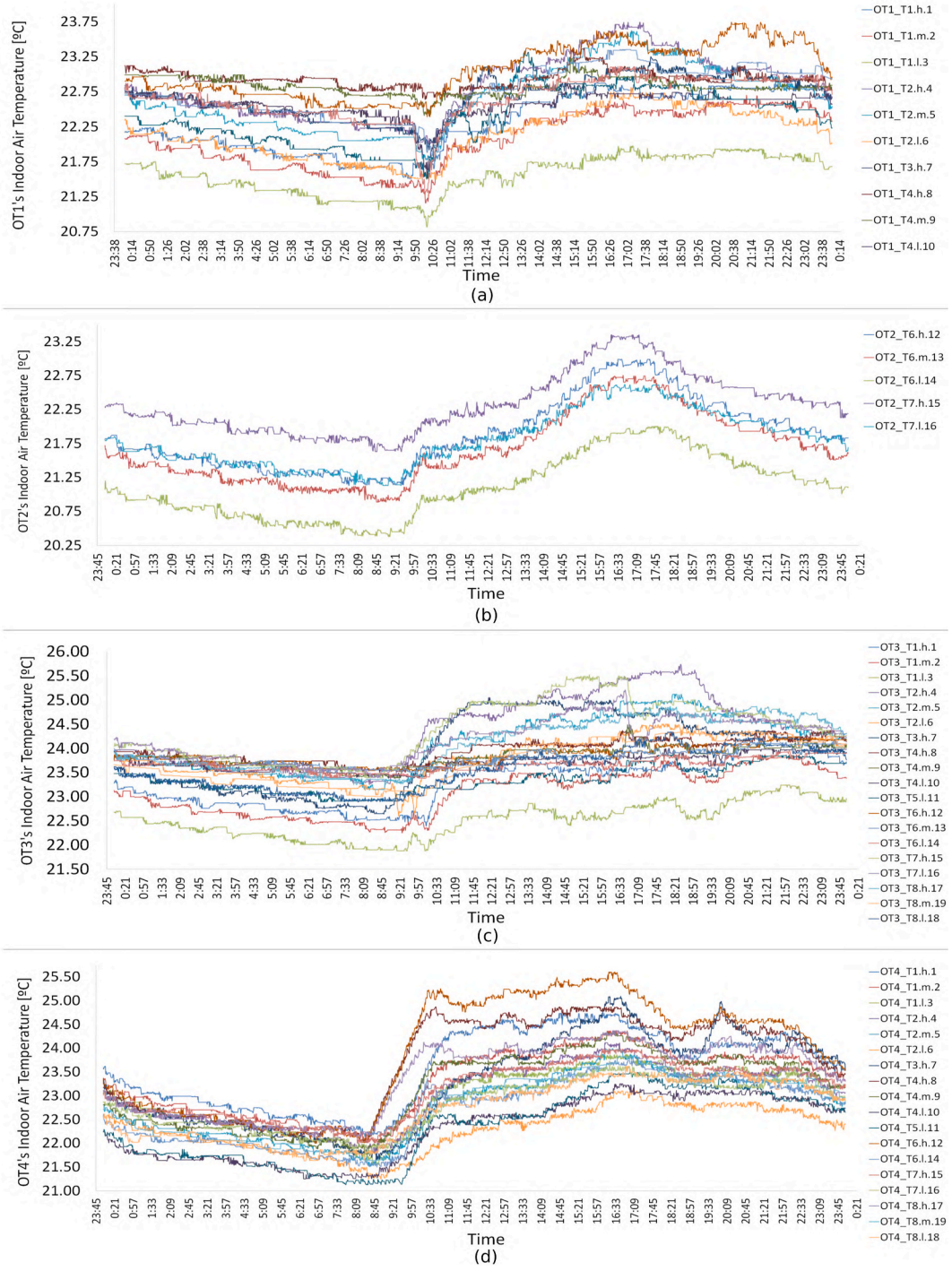

Fig. A4. Details of $\mathbf{T}_{dv_i}$ evolution during 24 h of data collected from the OT test ([22,23]): (a) OT1 data 11th of June 2019 from 0:00 to 24:00. (b) OT2 data of 11th of June 2019 from 0:00 to 24:00. (c) OT3 data of 29th of May 2019 from 0:00 to 24:00. (d) OT4 data of 24th of April 2019 from 0:00 to 24:00.

References

[1] «Energy Performance of Buildings», Energy - European Commission, 2014. https://ec.europa.eu/energy/en/topics/energy-efficiency/energy-performance-of-buildings. (Accessed 4 June 2019).

[2] «Europe's buildings under the microscope», BPIE - Buildings Performance Institute Europe. http://bpie.eu/publication/europes-buildings-under-the-microscope/. (Accessed 26 May 2020).

[3] Georgios Amanatidis, «Eurpean Polices on Climate and Energy towards 2020, 2030 and 2050», Policy Department for Economic, Scientific adn Quality of Life Polices, jun. 2019. Biefing PE 631.047, https://www.europarl.europa.eu/RegData/etudes/BRIE/2019/631047/IPOL_BRI(2019)631047_EN.pdf.

[4] G. Leijonhufvud, T. Broström, Standardising the indoor climate in historic buildings: opportunities, challenges and ways forward, J. Architect. Conserv. 24 (1) (Jan. 2018) 3–18, https://doi.org/10.1080/13556207.2018.1447301.

[5] F.J. Mesas-Carrascosa, D. Verdú Santano, J.E. Meroño de Larriva, R. Ortíz Cordero, R.E. Hidalgo Fernández, y A. García-Ferrer, Monitoring heritage buildings with open source hardware sensors: a case study of the mosque-cathedral of córdoba, Sensors 16 (10) (sep. 2016), https://doi.org/10.3390/s16101620.

[6] «ScienceDirect.com | Science, health and medical journals, full text articles and books». https://www.sciencedirect.com/. (Accessed 9 February 2020).

[7] «UNE-EN ISO 52016-1:2017. Energy performance of buildings - Energy needs for heating and cooling, internal temperatures and sensible and latent heat loads - Part 1: Calculation procedures.», Accessed: March 3, 2022, https://www.une.org/encuentra-tu-norma/busca-tu-norma/norma/?Tipo=N&c=N0059143.

[8] «ASHRAE Handbook: Fundamentals (2021)», Accessed: March 3, 2022, https://www.ashrae.org/technical-resources/ashrae-handbook/description-2021-ashrae-handbook-fundamentals.
[9] «ASHRAE Handbook: HVAC Applications (2019)», Accessed: Mars 3, 2022, https://www.ashrae.org/about/news/2019/ashrae-releases-new-hvac-applications-handbook.
[10] F.M. Baba, H. Ge, R. Zmeureanu, y L. (Leon, Wang, Calibration of building model based on indoor temperature for overheating assessment using genetic algorithm: methodology, evaluation criteria, and case study, Build. Environ. 207 (Jan. 2022) 108518, https://doi.org/10.1016/j.buildenv.2021.108518.
[11] D. Farmer, et al., Measuring thermal performance in steady-state conditions at each stage of a full fabric retrofit to a solid wall dwelling, Energy Build. 156 (dec. 2017) 404–414, https://doi.org/10.1016/j.enbuild.2017.09.086.
[12] R. Jack, D. Loveday, D. Allinson, y K. Lomas, First evidence for the reliability of building co-heating tests, Build. Res. Inf. 46 (4) (may 2018) 383–401, https://doi.org/10.1080/09613218.2017.1299523.
[13] D. Butler, A. Dengel, «Review of Co-heating Test Methodologies», NHBC Foundation, Knowhill, UK, 2013. https://www.nhbcfoundation.org/publication/review-of-co-heating-test-methodologies/.
[14] D. Wang, et al., Experimental study on coupling effect of indoor air temperature and radiant temperature on human thermal comfort in non-uniform thermal environment, Build. Environ. 165 (2019) 106387, https://doi.org/10.1016/j.buildenv.2019.106387, nov.
[15] P. Fornasini, The Uncertainty in Physical Measurements: an Introduction to Data Analysis in the Physics Laboratory, Springer Science+Business Media, LLC, New York, NY, USA, 2008.
[16] «BIPM - Guide to the Expression of Uncertainty in Measurement (GUM)». https://www.bipm.org/en/publications/guides/gum.html. (Accessed 4 February 2020).
[17] C. Giraldo-Soto, «Optimised Monitoring Techniques and Data Analysis Development for In-Situ Characterisation of the Building Envelope's Real Energetic Behaviour», Doctoral thesis, University of Bordeaux and University of Basque Country, 2021. http://www.theses.fr/2021BORD0041. (Accessed 26 July 2021).
[18] «Statistical functions (scipy.stats). Reference Guide». https://docs.scipy.org/doc/scipy/reference/stats.html?highlight=stats#module-scipy.stats. (Accessed 4 February 2020).
[19] «Pandas documentation». https://pandas.pydata.org/pandas-docs/stable/index.html#. (Accessed 4 February 2020).
[20] «Python.org», Python.org. https://www.python.org/. (Accessed 4 February 2020).
[21] «Affordable and Adaptable Public Buildings through Energy Efficient Retrofitting (A2PBEER)». http://www.a2pbeer.eu/. (Accessed 18 May 2018).
[22] C. Giraldo-Soto, A. Ekoreka, A. Barragan, y L. Mora, Dataset of an in-use tertiary building collected from a detailed 3D Mobile Monitoring System and Building Automation System for indoor and outdoor air temperature analysis, Data Brief (June 23, 2020) 105907.
[23] C. Giraldo-Soto, A. Erkoreka, A. Barragan, y L. Mora, «Data Repository. Dataset of an In-Use Tertiary Building Collected from a Detailed 3D Mobile Monitoring System and Building Automation System for Indoor and Outdoor Air Temperature Analysis», vol. 3, jun. 2020, https://doi.org/10.17632/fc2r9rdxbt.3.
[24] P. Wouters, L. Vandaele (Eds.), *The PASSYS Services. Summary Report of the PASSYS Project (EUR 15113 EN)*, European Commission. Directorate General XII for Science, Research & Development, 1994, ISBN 90-802301-1-1. Brussels, Belgium.
[25] C. Giraldo-Soto, A. Erkoreka, L. Mora, I. Uriarte, y L.A. Del Portillo, Monitoring system Analysis for evaluating a building's envelope energy performance through estimation of its heat loss coefficient, Sensors 18 (7) (jul. 2018) 2360, https://doi.org/10.3390/s18072360.
[26] «CO2, RH and T Room Transmitter for indoor applications». https://www.epluse.com/en/products/co2-measurement/co2-carbon-dioxide-transmitters/ee800/. (Accessed 5 January 2020).
[27] «Digital Humidity and Temperature Probe with Modbus RTU». https://www.epluse.com/en/products/humidity-instruments/humidity-measuring-modules/ee071/. (Accessed 5 January 2020).
[28] «Pasarelas – DEEI». https://deei.es/?product_cat=pasarelas. (Accessed 10 February 2020).